Title
Water Upconing in Underground Hydrogen Storage: Sensitivity Analysis to Inform Design of Withdrawal

Journal
Transport in Porous Media, 151(1)

ISSN
0169-3913

Authors
Oldenburg, Curtis M
Finsterle, Stefan
Trautz, Robert C

Publication Date
2023

DOI
10.1007/s11242-023-02033-0

Water Upconing in Underground Hydrogen Storage: Sensitivity Analysis to Inform Design of Withdrawal

Curtis M. Oldenburg[1*]
Stefan Finsterle[2]
Robert C. Trautz[3]

[1]Oldenburg PhD and Energy Geosciences Division, Lawrence Berkeley National Laboratory (LBNL), Berkeley, California
https://orcid.org/0000-0002-0132-6016

[2]Finsterle GeoConsulting, LLC, Kensington, California
https://orcid.org/0000-0002-4446-9906

[3]Electrical Power Research Institute (EPRI), Palo Alto, California

*Corresponding author. curto435@gmail.com

July 30, 2023

Abstract

The gas-water interface in Underground Hydrogen Storage (UHS) reservoirs creates the possibility that water will upcone to the well during hydrogen (H_2) withdrawal with detrimental impacts. We study the upconing of water to a hydrogen injection/withdrawal (I/W) well using both an analytical solution and numerical simulation. We carried out sensitivity analyses of the engineered properties (e.g., distance of well bottom to gas-water interface, withdrawal rate) and the intrinsic properties (e.g., reservoir permeability, porosity) of an idealized UHS system. Horizontal permeability is the main parameter controlling the height of upconing. Daily I/W cycles to some degree mitigate upconing because injection pushes down the gas-water interface. Sampling-based global sensitivity analyses show clearly that reservoirs with large horizontal permeability are preferred for avoiding upconing. Minimizing withdrawal rate and maximizing either the distance from well to gas-water interface or the length of the perforated well interval are important engineering controls to minimize upconing.

Keywords

Hydrogen storage, Underground Hydrogen Storage, Geological Hydrogen Storage, Upconing, Coning, Sensitivity Analysis

NOTE: This is the open access version of the paper. Citation to this work should be to

Oldenburg, C.M., Finsterle, S. & Trautz, R.C. Water Upconing in Underground Hydrogen Storage: Sensitivity Analysis to Inform Design of Withdrawal. *Transp Porous Med* **151**, 55–84 (2024). https://doi.org/10.1007/s11242-023-02033-0

1 Introduction

The use of hydrogen (H_2) as an energy carrier is being considered a potentially important component of the energy transition from fossil fuels to renewable energy sources. There are at least three reasons for considering H_2 in this context: (1) H_2 can be produced by electrolysis of water using abundant but intermittent renewable energy sources such as power from solar photovoltaic cells and wind turbines; (2) the conversion of H_2 into electrical or thermal energy by fuel cell or combustion does not result in production of greenhouse gases; and (3) H_2 generated by intermittent renewable sources can be stored for use upon demand over the course of a day, week, month, or season. Regarding (3), there are two obvious disadvantages that come with storing H_2, namely (i) the very low volumetric energy density of H_2 leads to the need for very large volumetric storage capacities and injection/withdrawal (I/W) rates, and (ii) there are losses in efficiency that come with interconversion of electricity and H_2.

One obvious approach to meet the challenges posed by the need to store large volumes of H_2 is to make use of the vast volumes of geologic formations for large-scale H_2 storage. For example, three solution-mined salt caverns have been used for storing H_2 in the U.K., and two have been used in the U.S. (Tarkowski and Czapowski, 2018; Mouli-Castillo et al., 2021). Other caverns have been used for storing other liquid and gaseous fuels (Plaat 2009; Arthur et al., 2017). While caverns can provide high deliverability (high withdrawal flow rates) and provide large storage volumes relative to surface tanks, they are not as abundant as natural gas reservoirs, nor do they have the volumetric capacity that exists in depleted natural gas reservoirs and natural gas storage sites that could be converted to hydrogen storage. Porous media brine-filled aquifers provide even more potential capacity for hydrogen storage.

Although cavern and porous media storage are both considered "geologic storage," flow and storage processes in caverns and porous media relevant to natural gas, H_2, and compressed air energy are very different. In short, gas storage in caverns occurs within a large open void with essentially a uniform pressure whereas storage in porous media is within the pore space of the rock and can occur across a pressure gradient (Oldenburg and Pan, 2013). Furthermore, storage in various kinds of caverns should also be distinguished by type of cavern (e.g., solution-mined cavern, mined cavern, abandoned mine) and not lumped into the overly simplistic term "geologic storage."

The widespread practice of underground (natural) gas storage (UGS) in porous media is a particularly close analogue to geologic H_2 storage. For this reason, we use the term underground hydrogen storage (UHS) in this paper. As used here, UHS refers to porous media formations with adequate porosity and permeability to facilitate storage and I/W, along with low-permeability caprock and lateral boundaries that provide sufficient sealing to store H_2 for the intended use case. A great deal of research is currently being conducted to assess the technical feasibility of UHS. Excellent older and very recent general information and review studies on UHS are available in the literature (e.g., Foh et al., 1979; Heinemann et al., 2021; Zivar et al., 2021; Wallace et al., 2021; Muhammed et al., 2022; Thiyagarajan et al., 2022).

Among the many concerns about technical feasibility of H_2 storage is coning of water upward from the gas-water interface (hereafter referred to as upconing) (Sainz-Garcia et al., 2017; Luboń and Tarkowski, 2020). Upconing of water can lead to the need for water separation at the surface and interfere with gas flow in the well, and delivery from the storage facility. With underground natural gas storage (UGS) in porous media being successfully carried out for over 100 years (Katz and Tek, 1981; Knepper, 1997), the question arises as to why upconing is such a concern for UHS and apparently not a universal concern for UGS. The first-order reason is that H_2 has approximately one-third the energy density by volume compared to CH_4, resulting in the need to inject or extract larger volumes of H_2 potentially over shorter periods of time than is the case for CH_4 in seasonal UGS, other differences in the transport and combustion properties of the two gases notwithstanding (e.g., Zhao et al., 2019). This need to withdraw larger volumes of H_2 relative to natural gas (CH_4) is true for both seasonal and daily use cases because of the lower energy density by volume of H_2. Insofar as seasonal storage will involve both large withdrawal rates and potentially month(s)-long withdrawal periods, upconing is expected to be a serious concern. Regarding the duration of withdrawal, upconing does not necessarily cause monotonic rise in the gas-water interface until it encounters the well. Rather, there can be steady-state configurations with a quasi-steady upconed mound of groundwater that does not intersect the well. Therefore, the period of withdrawal may or may not be significant for ultimate water entry into the well due to upconing. The experiences of 100+ years of UGS which largely serves seasonal use cases, will certainly be able to inform nascent UHS activities in the area of upconing.

In this paper, the term upconing describes the upward movement of water (aqueous phase) from the gas-water interface due to withdrawal of gas from the gas cap through a well. Upconing is caused by the low pressure created outward from the perforations of a gas well under withdrawal. The result of withdrawal of gas is the flow of mobile gas and water from above, the side, and below the well toward the well screen. Water withdrawn with H_2 is a problem for UHS because withdrawn H_2 needs to be as pure as possible—entrained liquid water would need to be separated, and vapor would likely need to be condensed and separated. In addition, too much water getting into a well can "kill" the well, i.e., stop gas from flowing freely up the well (Falcone and Barbosa, 2013). In short, upconing of water into a UHS extraction well needs to be avoided.

The purpose of this paper is to elucidate the phenomenon of water upconing in the context of UHS and make recommendations on how it can be minimized. We address two specific questions:

1. Under what reservoir and operating conditions is upconing a potential problem for UHS?

2. What is the relative importance of the various reservoir properties and operating conditions for water upconing?

Using both analytical solution and numerical simulation approaches, we perform sensitivity analyses to determine the reservoir properties and operational controls that most strongly influence upconing. We use highly idealized and simplified reservoir geometries and properties so that the results can be used to select and design favorable aspects of generalized UHS systems and to identify use cases that minimize water upconing. A sketch of upconing is shown in Figure 1 along with the important parameters that control it.

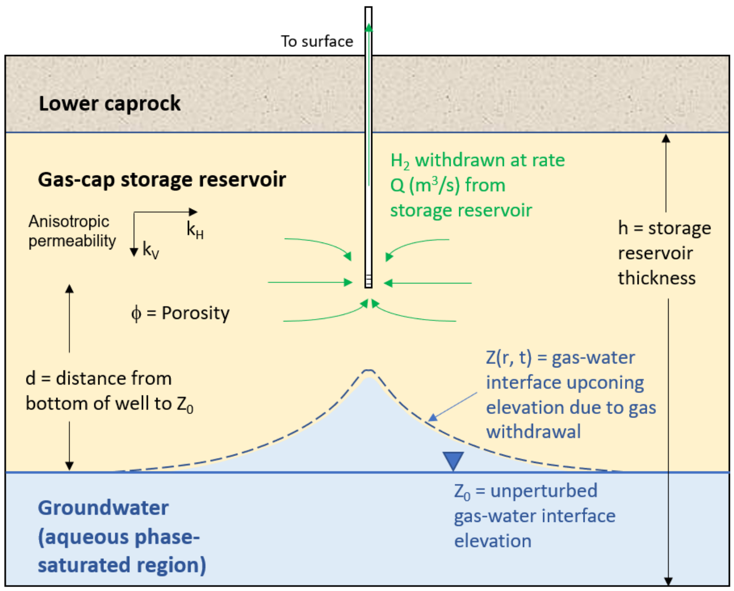

Figure 1. Sketch of idealized porous media UHS system showing one I/W well along with gas-water interface elevation (Z) rising as a function of radius (r) and time (t) from its initial position to an upconed configuration during gas withdrawal along with parameters ϕ, k_H, k_V, Q, and d.

2 Background and Prior Work

A great deal of work has been done in the area of upconing in the context of subsurface fluid extraction carried out using wells. Specifically, in the groundwater resources and hydrology field, coning of salty or briny water upward into overlying freshwater extraction wells installed near ocean coastlines has been addressed starting many decades ago (Muskat and Wycoff, 1935; Dagan and Bear, 1968; Chandler and McWhorter, 1975) and is continuing to the present with the advent of horizontal wells (Sun and Wong, 2017). In the oil and gas industry, coning can be more complex, with instances of simultaneous downward coning of overlying gas into oil extraction wells, and upward coning of water into the same oil well (e.g., Johns et al., 2005). Briefly, in hydrocarbon recovery, there is only one (long) withdrawal period and natural gas components are highly soluble in oil. Because of this, the need for gas-oil and water separation at the surface (e.g., in a frac tank) is very common. Such separation serves the purpose of isolating the desired phase(s) for sale on the market regardless of the processes leading to the multiple phases (e.g., depressurization, downconing of gas, or upconing of water). In contrast, UHS involves multiple I/W cycles potentially with alternating upconing and downconing of water with low H_2 solubility.

Coning has also been studied in the context of leakage of CO_2 through wells by development and application of a semi-analytical solution for upconing of water into wells leaking CO_2 from carbon sequestration sites (Nordbotten and Celia, 2006). In addition, upconing was analyzed in the context of compressed air energy storage in porous media (Wiles and McCann, 1981). The importance of upconing for UHS was emphasized by Sainz-Garcia et al. (2017) and Luboń and Tarkowski (2020).

For our purposes, the transient analytical solution of Dagan and Bear (1968) will be shown to be very useful. In their solution, the amount of upconing, as quantified by the rise of a sharp saltwater-freshwater interface, depends on time, radius (lateral distance away from the well), the intrinsic properties of porosity, horizontal and vertical permeability, and the fluid densities and viscosities. The key operational parameters are extraction rate and distance from the bottom of the well to the original interface.

Because the freshwater-brine system considered by Dagan and Bear (1968) is fully saturated, capillary pressure and relative permeability are immaterial and are not considered in the analytical solution. We show below that despite the lack of consideration of two-phase flow mechanisms and the fact that Dagan and Bear (1968) developed and validated their solution for two fluids (salty and fresh water) with relatively modest differences in density and viscosity, their solution matches reasonably well with numerical simulations of two-phase systems with fluids that have large differences in density and viscosity, namely H_2 above fresh water. In this study, we utilize the Dagan and Bear (1968) analytical solution and the numerical simulation and sensitivity analysis methods implemented in iTOUGH2 (Finsterle et al., 2017), which incorporates the multi-phase and multicomponent forward simulator TOUGH2 (Pruess et al., 2012) and the equation of state module EOS7CH (Oldenburg and Finsterle, 2023), which was specifically developed to simulate UHS reservoirs.

3 Methods

3.1 Analytical Solution and Sensitivity Analysis

For simple and fast estimates of upconing, we use the Dagan and Bear (1968) analytical solution (hereafter referred to as the DB model). The DB model was developed to calculate the shape and maximum height of the upconed interface between salty water subjacent to fresh water that develops when fresh water is pumped up a well not far from the interface. Their solution used the method of small perturbations to develop a linearized equation for the motion of the sharp interface between the two liquids. The DB model allowed for dipping aquifers and results were validated against laboratory experiments by Dagan and Bear (1968).

In radial coordinates, the DB model equations for the interface position Z as a function of radius (r) away from the well and time was clearly presented for a horizontal aquifer by Sun and Wong (2017) as

$$Z(r,t) = \frac{Q}{2\pi\left(\frac{\Delta\gamma}{\gamma}\right)K_x d}\left[\frac{1}{\left(1+R'^2\right)^{\frac{1}{2}}} - \frac{1}{\left[(1+\gamma')^2+R'^2\right]^{\frac{1}{2}}}\right] \tag{1}$$

where the intermediate terms R' and γ' are given by

$$R' = \frac{r}{d}\left(\frac{K_z}{K_x}\right)^{\frac{1}{2}} \tag{2}$$

$$\gamma' = \frac{\frac{\Delta\gamma}{\gamma}K_z}{2\phi d}t \tag{3}$$

and symbols are defined in Nomenclature. Briefly, Equations 1–3 show that the shape of the interface ($Z(r,t)$) depends on the volumetric fluid withdrawal rate (Q), the densities (γ) of the two fluids, the conductivities in the r- and y-directions (K_x (= K_r) and K_y), the vertical distance d between the extraction point and the initial elevation of the interface (d), porosity (ϕ), radius (r), and time (t) (see also Figure 1). Eq. (1) is at most an approximation of the rise of water before it reaches the critical condition when the upconed water intersects the bottom of the well.

We use Excel to calculate $Z(r,t)$ by the DB model equations. Density and viscosity of H_2 gas and aqueous phase water are calculated in Excel using the CoolProp add-in (Bell et al., 2014). For sensitivity analysis using Monte Carlo methods, we use a free Excel add-in called Argo (BoozeAllen, 2023).

Although developed and validated by Dagan and Bear (1968) for a sharp interface between two fluid mixtures (salty water below fresh water) of a single phase (no capillary pressure) with relatively small density contrast, it will be shown below that Eqs. 1–3 provide usable estimates of the upconing of water below a hydrogen withdrawal well in a UHS reservoir where the density of H_2 is approximately 7 kg m^{-3} and water is 1000 kg m^{-3}. The simple DB model serves as a complement to the fully coupled TOUGH2 numerical simulations and provides a fast sensitivity analysis capability. Used carefully, the DB model offers a simple and fast tool that can aid in the design of UHS systems to avoid upconing.

3.2 Numerical Simulation with Sensitivity Analysis

For predictive modeling and sensitivity analyses of the fully coupled non-linear equations describing mechanisms of I/W and gas-liquid fluid flow in UHS, including mechanisms related to upconing, we use iTOUGH2 (Finsterle et al., 2017; Finsterle, 2022) and EOS7CH (Oldenburg and Finsterle, 2023). EOS7CH is an equation of state module for water and non-condensible gas (NCG) mixtures of any gas pair within the system hydrogen (H_2), methane (CH_4), carbon dioxide (CO_2), and nitrogen (N_2) with or without an aqueous phase and H_2O vapor. EOS7CH is an extension of EOS7C (Oldenburg et al., 2004; Pruess et al., 2012) and adds the RefProp (Lemmon et al., 2018) subroutines for estimating real gas-mixture properties to the prior three choices of cubic equations of state (Peng-Robinson, Redlich-Kwong, and Soave-Redlich-Kwong). EOS7CH can model two-phase flow and transport of gaseous and aqueous phases over a wide range of pressures and temperatures encountered in aquifers and subsurface natural gas reservoirs. Gas mixture density, enthalpy, and viscosity are calculated by any one of the four real gas properties modules as chosen by the user. Solubility of the NCG and base gas (BG) in the aqueous phase is calculated using a fugacity-based approach. Mass transport of the gaseous and dissolved components is by advection and Fickian molecular diffusion.

4 Use Case

4.1 Definitions

In general, before any modeling or simulation of UHS is carried out, a choice of storage use case must be made. In short, the use case is the intended purpose of any given UHS endeavor. The use case establishes (controls) the operating parameters and requirements of the UHS system. In Figure 2, we show the aspects of UHS that need to be defined/chosen to establish a use case. A use case definition involves characterizing the production, transportation, and storage of H_2, as well as aspects of the withdrawal and use. Figure 2 is meant to be representative of the basic aspects of UHS rather than comprehensive in the range or scope of properties.

As shown in Figure 2, the use case description starts in the upper left-hand side with definition of the method and energy source used for H_2 production, proceeds through how H_2 is transported to the UHS site, and includes the injection schedule and rates in the injection wells. On the right-hand side, there is withdrawal of H_2 from the storage reservoir, and its use, e.g., potentially making electricity on-site by means of a fuel cell or combustion, or transport off-site for various uses. The aspects of the use case in the upper (blue) part of the figure are above-ground and can be engineered and designed for economic and technical feasibility. In the subsurface (lower part of Figure 2), there are various storage reservoir and trap types which are largely pre-determined by natural processes and difficult if not impossible to change. The I/W schedules must be designed to match the restrictions and opportunities provided by the underground storage resource.

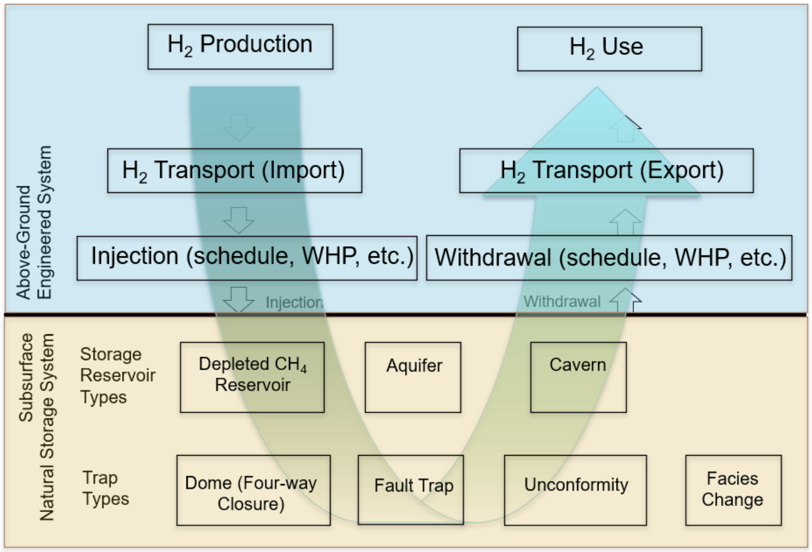

Figure 2. Sketch of fundamental aspects of a UHS use case showing the above-ground engineered parts of the use case that need to be designed to match the limitations of the underground storage resources.

4.2 Use Case: Green Hydrogen Produced Daily

Here, we consider a use case—applicable to a region such as California (USA)—in which H_2 is produced for six hours each day by hydrolysis using renewable electricity provided primarily by solar photo-voltaic (PV) sources (referred to as "green hydrogen"). During six hours each day of strong insolation, H_2 produced at the UHS site (using otherwise curtailed renewable electricity from the grid) is injected into the porous media UHS reservoir. As the sun sets and the renewable electricity supply diminishes, demand rises as people return home from work and turn on appliances and air conditioners. During this late afternoon and evening period, H_2 is withdrawn from the reservoir and used in on-site fuel cells or gas turbines for conversion back into electricity which is exported to the grid.

Figure 3 shows the rates of electricity supply and demand along with the hypothetical H_2 I/W schedule for the chosen use case for a generic sunny day in California. The electricity generation (supply) curves for California for any current day can be viewed at https://www.caiso.com/TodaysOutlook/Pages/supply.aspx. Figure 3 shows the instantaneous power on the *y*-axis plotted against the hours of the day on the *x*-axis for a day with excellent solar PV power production as shown by the green curve. We have superimposed the blue step function curve showing the I/W schedule of the chosen use case. Specifically, the UHS use case we consider here involves six hours of H_2 injection into the storage reservoir from 10 AM to 4 PM, followed by six hours of withdrawal from 4 PM to 10 PM. This daily I/W cycle is followed by 12 hours of well shut-in.

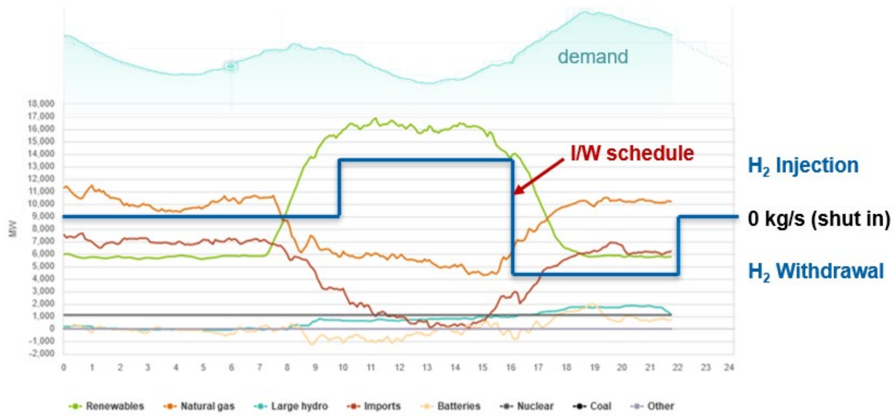

Figure 3. Instantaneous electricity supply (MW) curves for various renewable energy sources plotted over the hours of a day in California showing also the demand curve (top-most curve), and the UHS use case assumed here (heavy blue line) involving six hours of injection, six hours of withdrawal, and 12 hours of shut-in.

Note that no scale is provided in Figure 3 for the I/W because it varies by month and day throughout the year, the overall availability of H_2 as well as the number of wells used in the UHS system. To get an idea for what the H_2 I/W rates would be for the chosen use case, we looked at data for California where in April 2022, 6×10^5 MWh of electricity were curtailed which is equivalent to 2×10^7 kWh/d (CalISO, 2022). Assuming advances continue and a 95% efficient electrolyzer is available using 41.5 kWh to produce 1 kg H_2 (Blain, 2022), 4.82×10^5 kg H_2/d could be produced which would come to an injection rate of 22.3 kg H_2/s over the six hours of the day when electricity is curtailed. Assuming a storage site with four I/W wells, this would be approximately a 5.5 kg H_2/s injection per well for six hours per day.

Below, we present modeling and simulation results to address the key questions posed in the study regarding what operational parameters and reservoir properties control upconing during withdrawal for this assumed use case. We examine systems with increasing complexity, starting with two fluids of similar density and viscosity, and then we move to more complex systems with two-phase flow of H_2 and water. We start by simulating a single withdrawal event from a point-source well, and later simulate a more realistic vertical well with I/W over multiple cycles.

5 Comparison of Analytical Model and Numerical Simulation of Upconing

5.1 Introduction

In this section, we present results from the DB model and numerical simulations for water-brine and H_2-water systems. The purpose is to demonstrate the utility of the single-phase DB analytical solution for modeling upconing even for applications involving two-phase systems. We solve the DB model Eqs. 1–3 in Excel and make use of the CoolProp add-in (Bell et al., 2014) for estimating density and viscosity of H_2. We simulate idealized systems with domains and boundary conditions designed to emulate the simple DB-model assumptions.

5.2 Water-Brine System

We begin with a single-phase aqueous water-brine upconing scenario similar to the one for which the DB model was developed. Essential properties of the system are shown in Table 1. The domain and boundary conditions of an idealized aquifer system with two stratified fluids of different densities is shown in Figure 4. The top, bottom, and right-hand (outer radial) boundaries are held at constant conditions, consistent with the infinite aquifer assumption of the DB model. As shown in Figure 4, the domain was discretized in the Z-direction with a graded mesh refined around the I/W well (Z = - 40 m) using 48 rows of grid blocks, and in the R-direction using two equal-spaced columns each 0.031 m in radius at the center of the radial system (left-hand side) and then logarithmic spacing out to 100 m, totaling 52 columns of grid blocks. Note that we distributed the -25 kg/s mass sink scaled by grid-block volume among six grid blocks in the near-well region to avoid excessive local drawdown that may approach non-physical negative pressures.

Table 1. Properties of the water-brine upconing comparison case.

Properties of the Water-Brine Upconing Problem	
Thickness and extent of the domain	100 m, 100 m
Porosity (ϕ)	0.10
Permeability (k_H)	1.0×10^{-12} m^2
Permeability (k_V)	1.0×10^{-12} m^2
Distance from well to freshwater-brine interface (d)	10 m
Extraction rate of fresh water (Q, Q_m) distributed within six grid blocks around the well level at Z = -40 m)	-0.025 m^3 s^{-1} , -25 kg s^{-1}
Density of brine (@ 100 bar, 40 °C)	1050 kg m^{-3}
Density of fresh water (@100 bar, 40 °C)	996.7 kg m^{-3}
Viscosity of brine (@100 bar, 40 °C)	1.29×10^{-3} Pa s
Viscosity of fresh water (@100 bar, 40 °C)	6.52×10^{-4} Pa s

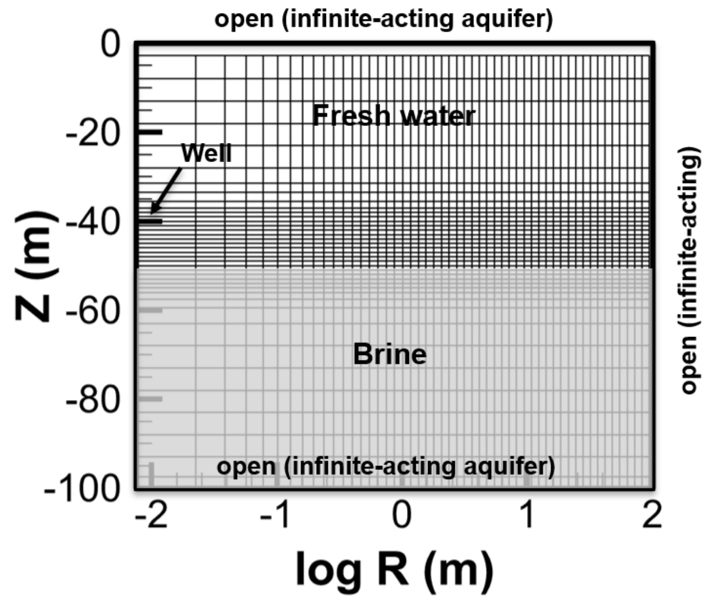

Figure 4. (a) Two-dimensional radial (RZ) domain, discretization (the lines show connections), and boundary conditions for testing TOUGH2 simulations of water-brine upconing against the DB model. The brine layer is represented by the light gray color.

Simulation results of upconing of brine into a freshwater layer from iTOUGH2 (using TOUGH2 as its forward model) are shown in Figure 5. Simulation results of the 0.5 isopleth of brine mass fraction and the DB model brine interface are in fair agreement at t = 4 hrs and 6 hrs, with upconing slightly less in the simulation results than in the DB model. The shapes of the 0.5 isopleth and interfaces agree well in the two models.

It is important to point out that the DB model and iTOUGH2 differ in that the DB model is a sharp-interface model whereas TOUGH2 is modeling a continuously variable brine mass fraction in the aqueous phase, resulting in a continuously variable density field. Note that the TOUGH2 results are plotted by the aqueous brine mass fraction isopleth equal to 0.5 (even though the brine mass fraction field is actually smeared as shown in Figure 5e), along with liquid flow direction vectors. This inherent smearing by the numerical model is one reason for the smaller upconing of TOUGH2. Specifically, as denser brine upcones and is withdrawn at a constant mass flow rate, the volumetric withdrawal is less leading to less pressure drawdown and less upconing. The smearing and dilution of the upward-moving brine plume is enhanced by converging flow as fresh-water flows in radially from the sides at the same time brine is pulled upwards from below to the well.

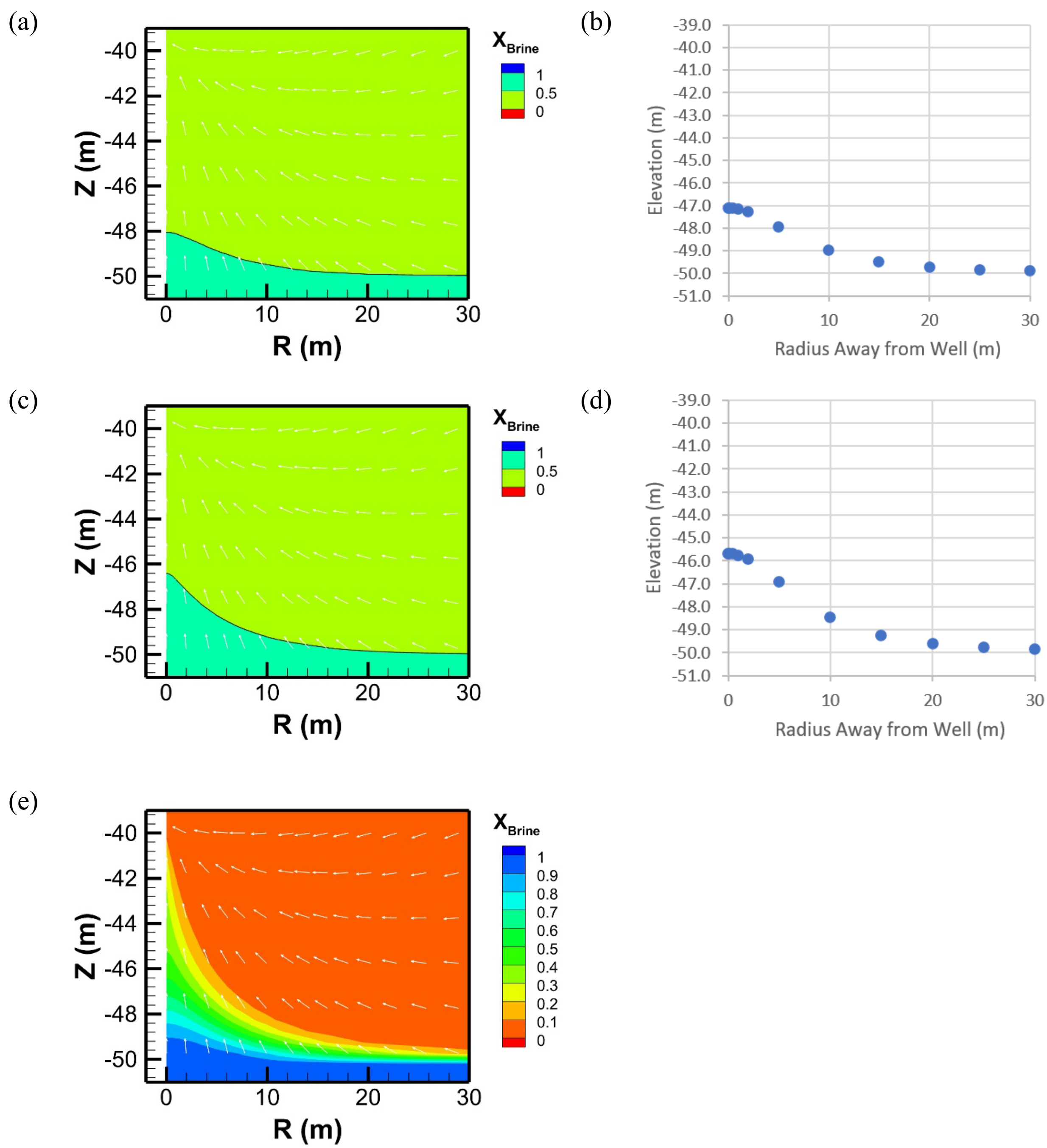

Figure 5. Results of a water-brine upconing problem. (a) TOUGH2 results as shown by the 0.5 isopleth of brine mass fraction at t = 4 hrs, (b) DB model results at t = 4 hrs, (c) TOUGH2 results at t = 6 hrs, and (c) DB model results at t = 6 hrs. Frame (e) shows the TOUGH2 model results at t = 6 hrs for multiple contours of the brine mass fraction.

5.3 H_2-Water System

The second comparison is between iTOUGH2-EOS7CH simulations of two-phase H_2 withdrawal and the single-phase DB model. The parameters of the case are given in Table 2. The small differences in the densities and viscosities shown in the table occur because of differences in the equations of state used for the DB model input in Excel and in EOS7CH, and because the DB model assumes pure fluids whereas phases may be impure (mixtures of multiple components) in our simulations. Owing to the preference by potential UHS operators for high-porosity and high-permeability reservoirs, it is justifiable to neglect capillary pressure in the numerical simulations given the low P_{cap} values expected for clastic sandstones. Another property of two-phase systems not present in the single-phase DB model, but important in the two-phase simulation, is relative permeability (k_{rel}). A linear relative permeability relation with S_{lr} = 0.99 tends to sharpen a liquid phase front, and we use that approach here for comparison against the DB model results, which assumes a sharp interface between the two fluids.

Although recent studies have elucidated hysteretic behavior of k_{rel} in H_2-water systems (Lysyy et al., 2022; Bo et al., 2023; Jangda et al., 2023), we assume non-hysteretic k_{rel} in this study. Hysteresis will certainly impact two-phase flow during upconing (imbibition) and downconing (drainage) around the gas-water interface and potentially lead to trapping of H_2 in around the gas-water interface with impacts on efficiency of extracting gas. But our focus is on preventing or controlling upconing rather than storage efficiency or trapping of H_2. The fundamental cause of upconing is the pressure drawdown that occurs at the well during gas withdrawal. As we will show in this study, drawdown at the well is influenced mostly by how easily gas can flow to the well from the side (as controlled by horizontal permeability) and by the rate that gas is being withdrawn. Upconed water, and the associated flow and trapping processes attending hysteretic effects, need to be kept far enough away from well perforations that they do not negatively impact UHS operations. Our study is focused on defining the intrinsic reservoir properties and operational parameters that are critical for avoiding this upconing of water to the well.

The domain and boundary conditions for this comparison case are shown in Figure 6. We discretized the domain in the *Z*-direction with a graded mesh refined around the I/W level using 72 rows, and in the *R*-direction two equally spaced columns each 0.031 m in radius at the center (left-hand side) and then logarithmic spacing out to 100 m, totaling 52 columns. Note the open (infinite aquifer) boundary conditions on the bottom and right-hand side are chosen to match assumptions of the DB model rather than for realism relative to UHS in confined aquifers or depleted gas reservoirs. Note also that for the comparisons against the DB model in this section, we simulate withdrawal only and the initial condition is a flat-lying gas-water interface. In a later section of the paper, we present an injection and withdrawal cycle and discuss the implications and sensitivity relative to minimizing upconing for the six-hour I/W use case.

Table 2 (corrected). Properties of the H_2-water upconing system for comparison against the DB model.

Property	DB model	Used for TOUGH2
Gas cap thickness, total reservoir thickness, and radial extent (outer radius) of the reservoir	infinite, infinite, infinite	50 m, 100 m (with open boundary at bottom), 100 m (open boundary condition)
Porosity (ϕ)	0.10	0.10
Permeability (k_H)	1.0×10^{-12} m^2	1.0×10^{-12} m^2
Permeability (k_V)	1.0×10^{-12} m^2	1.0×10^{-12} m^2
Relative permeability (k_{rel})	Not applicable	Linear with S_{lr} = 0.99
Distance from well to H_2-water interface (d)	10 m	10 m
Extraction rate of rate of H_2 (Q_m)	-5.5 kg s^{-1}	-5.5 kg s^{-1}
Density of water	996 kg m^{-3}	996 kg m^{-3}
Density of H_2	7.32 kg m^{-3}	7.87 kg m^{-3}
Viscosity of water	6.54×10^{-4} Pa s	5.11×10^{-4} Pa s
Viscosity of H_2	9.31×10^{-6} Pa s	9.53×10^{-6} Pa s

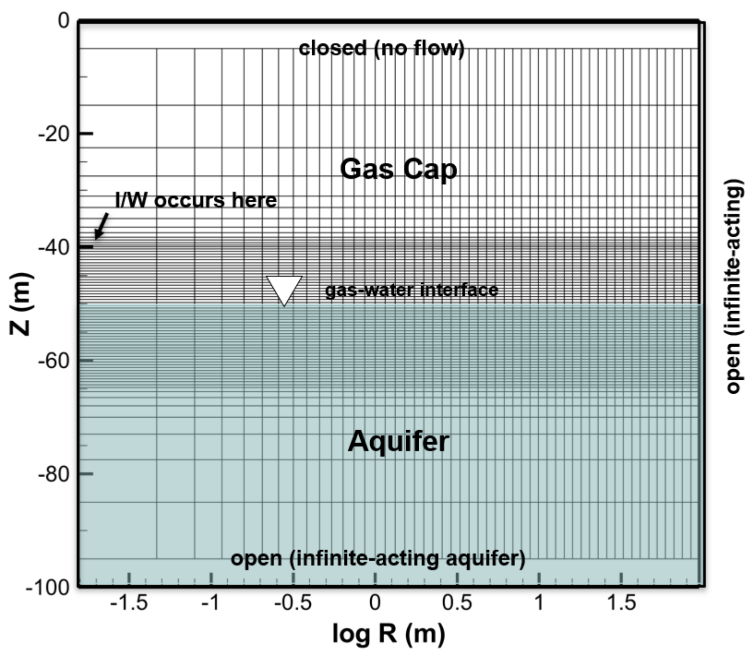

Figure 6. Two-dimensional radial (RZ) domain, boundary conditions, initial aquifer (blue) and gas cap regions, and discretization (lines show connections) for testing against the DB model.

Figure 7 shows the TOUGH2 results of water upconing arising from H_2 withdrawal at -5.5 kg/s on the left-hand side (center of the *RZ*) at *Z* = -40 m. Note that we distributed the -5.5 kg/s mass sink scaled by grid-block volume among four grid blocks in the near-well region to avoid excessive local drawdown in the highly refined discretization at the well. The simulation results show that water upcones to a height of approximately 3 m. Note from the temperature field that the H_2 heats up slightly as it decompresses moving toward the extraction point (Figure 7c) due to the negative Joule-Thomson coefficient of H_2. Finally, Figure 7d shows that the DB model predicts 5.6 m of upconing and an upconed region that is broader than the TOUGH2 result.

The DB model is parameterized using volumetric withdrawal of an incompressible liquid (water) whereas in this UHS system it is highly compressible H_2 that is being withdrawn at a constant mass rate. The drawdown caused by gas withdrawal is less for a compressible gas because gas expansion during withdrawal suppresses the pressure drop.

Overall, the TOUGH2 simulation is modeling more processes and mechanisms (e.g., pressure-dependent densities, relative permeability effects) than are accounted for in the single-phase DB model. We conclude from this comparison that the DB model can only approximately represent upconing for this H_2-water system. This result illustrates that the DB model provides only a first-order approximation of water upconing in UHS systems, and that numerical simulations are needed to accurately model the details of upconing in UHS systems.

This is the open access version of a published paper. Please see pg. 1 for how to cite this paper.

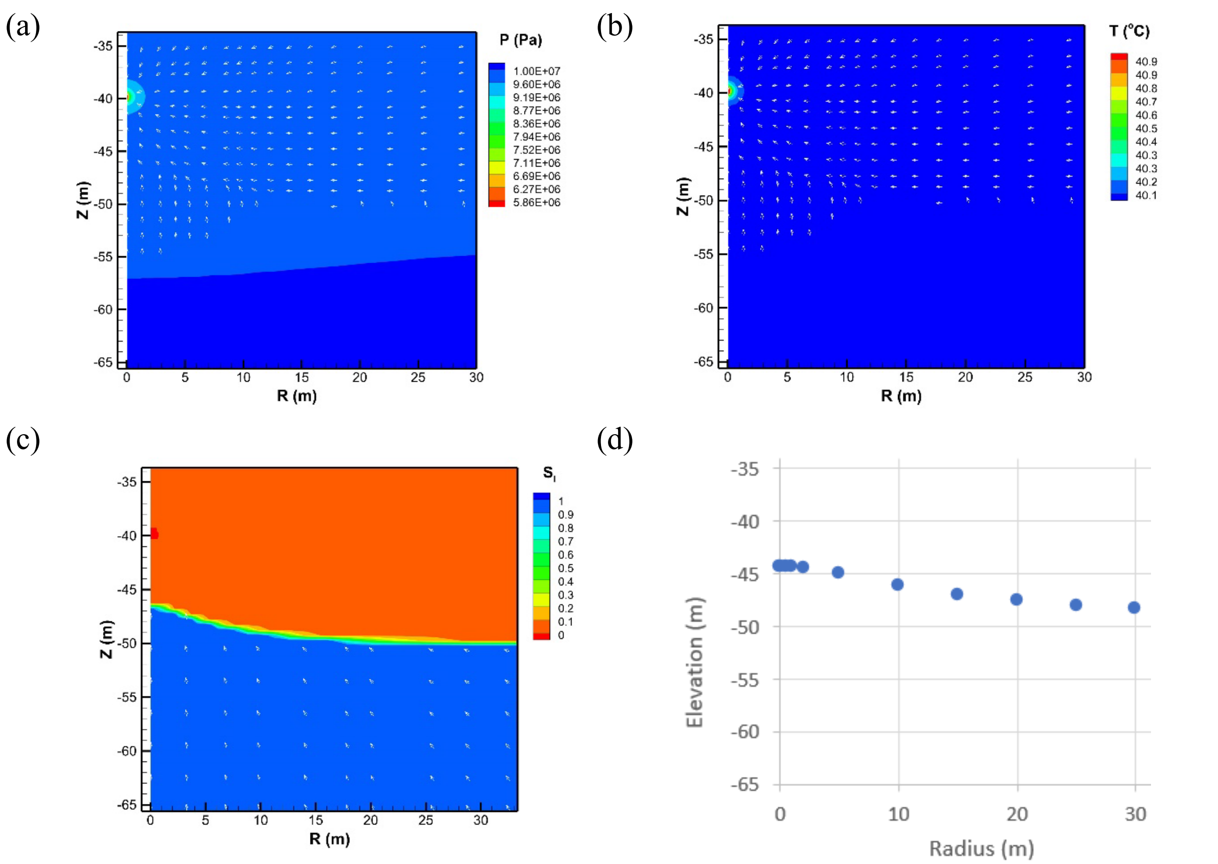

Figure 7. Simulation results of water upconing after 6 hrs of withdrawal show TOUGH2 results of (a) pressure and gas flow direction vectors, (b) temperature and gas flow direction vectors, and (c) liquid saturation and liquid flow direction vectors. Frame (d) shows the DB model result.

6 Simulation of UHS Upconing in a Generic Reservoir System

6.1 Domain and Discretization

To more accurately assess upconing in UHS and carry out sensitivity analyses, we next move away from the DB model assumptions while still using a simplified generic 2D radial (*RZ*) system. Although the UHS system is still highly idealized both in geometry and properties (e.g., horizontal and homogeneous), our model simulates fully coupled flow and transport processes based on state-of-the-art equations of state to estimate fluid properties (Oldenburg and Finsterle, 2023). The domain and boundary conditions are shown in Figure 8. We discretized the domain in the *Z*-direction using 77 rows 0.5 m thick with a local refinement (0.25 m-thick layer) at the I/W depth for a total of 81 rows, and in the *R*-direction we used two equal-spaced columns each 0.031 m in radius at the center (left-hand side) and then with logarithmic spacing out to 100 m totaling 52 columns. We carry out I/W into two radial grid blocks with rates scaled by grid-block volume for an effective well radius of 0.062 m.

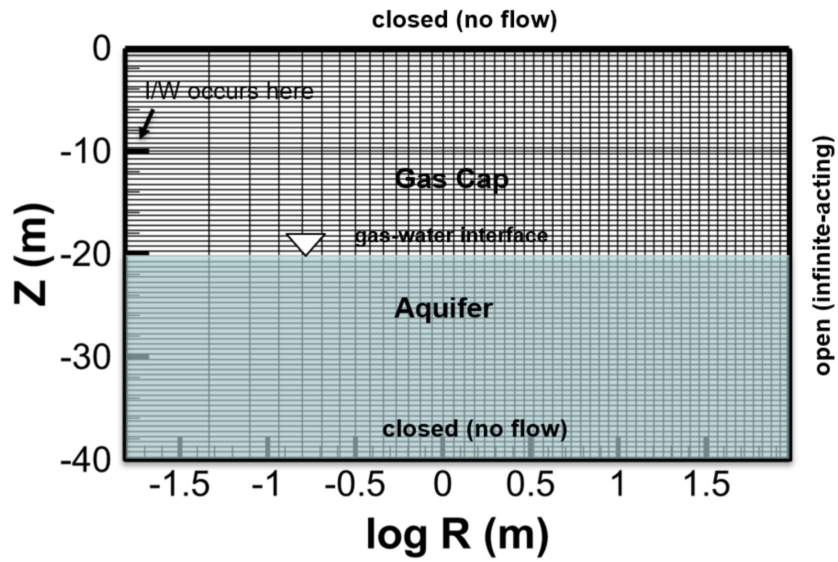

Figure 8. Two-dimensional radial (RZ) domain, boundary conditions, and discretization (lines show connections) for a generic single-well two-phase system showing initial gas and aquifer (blue) regions in the reservoir.

6.2 Properties of the UHS System

The properties of the reservoir and well for the generic UHS system modeled below are provided in Table 3. Because the reservoir rock assumed here is a coarse sandstone, capillary pressure effects are small and we assume P_{cap} is zero. The parameters of the van Genuchten model (Luckner et al., 1989) for k_{rel} are presented in Table 3. Molecular diffusion fluxes in TOUGH2 are calculated using diffusion coefficients such as those shown in Table 3 along with several other multipliers (Pruess et al., 2012). Although all of our simulations are carried out non-isothermally and some interesting thermal effects are observed, the magnitude of these effects is small and not significant from an operational perspective.

As described in an earlier section, the use case scenario involves a daily cycle of injection of H_2 for six hours at a constant rate into the reservoir which is initially at a hydrostatic pressure of approximately 10 Mpa (100 bars) and a temperature of 40 °C. This is followed by six hours of withdrawal of mass from the reservoir, which is followed by 12 hours of well shut-in.

Table 3. Reservoir properties for the generic UHS system.

Reservoir Properties	
Thickness and extent (radius) of the reservoir	40 m, 100 m (open boundary)
Depth of top of reservoir	1000 m
Initial pressure at bottom of gas cap	10 Mpa
Initial temperature	40.0 °C
Porosity (ϕ)	0.10
Permeability (k_R)	1.0×10^{-12} m^2
Permeability (k_V)	1.0×10^{-12} m^2
Pore compressibility	1×10^{-10} Pa^{-1}
Thermal conductivity of water-saturated reservoir formation	2.50 W/(m K)
Heat capacity (C_P) of saturated reservoir	1000 J/(kg K)
Relative Permeability (k_r) Modified van Genuchten (Luckner et al. (1989) k_r model $S_{el} = \frac{S_l - S_{lr}}{1 - S_{lr}}$ $S_{eg} = \frac{S_l}{1 - S_{gr}}$ $k_{rl} = S_{el}^{\eta} \cdot \left[1 - \left(1 - S_{el}^{1/m}\right)^m\right]^2$ $k_{rg} = \left(1 - S_{eg}\right)^{\xi} \left(1 - S_{eg}^{1/m}\right)^{2m}$	$S_{lr} = 0.076$ $S_{gr} = 0.10$ $m = 0.7$ $\eta = 0.5$ $\xi = 1/3$
Initial saturation	Aqueous phase at residual gas saturation (0.076) in the gas cap, with gas-water interface at $Z = -20$ m
Molecular binary diffusion coefficient (D)	1.0×10^{-5} m^2 s^{-1} (gas phase) 1.0×10^{-10} m^2 s^{-1} (aqueous phase)

6.3 *Numerical Simulation of Injection and Withdrawal*

We show results of a single injection and withdrawal (I/W) cycle (24 hours) with focus on the motion of the gas-water interface. The initial conditions of the system are gas-static pressure above a sharp gas-water interface at $Z = -20$ m, with hydrostatic pressure below, constant temperature of 40 °C, and a hydrogen-filled pure gas head space above a single-phase aqueous region.

For the simulations of I/W, we distributed the source/sink terms scaled by grid-block volume among four grid blocks along the left-hand side at the well location. As with the DB-like UHS case shown previously, this use of four grid blocks instead of one for I/W arose from the strong local drawdown in pressure that occurs when withdrawal is from one small "well" grid block; by distributing the mass extraction among four grid blocks, the drawdown around the "well" is less. While approaching a vacuum is not an issue during the injection period, for consistency we use the same four grid blocks for both injection and withdrawal.

Figure 9 shows simulated results of the pressure, temperature, saturation, and gas density fields following six hours of injection of 40 °C H_2 at 5.5 kg s^{-1}. For visualization, we show results only for a portion of the domain out to R = 30 m because conditions are largely unchanged in the rest of the domain. As shown, injection increases the pressure in the near-well region. Gas velocity directions are shown by the uniform-length arrows in Figure 9a. Interesting non-isothermal effects are evident in Figure 9b. The small heating and cooling effects are likely arising from a combination of Joule-Thomson and latent heat effects from evaporation/condensation of water. Figure 9d shows that the main effect of downconing is the push down of the gas-water interface as H_2 is injected.

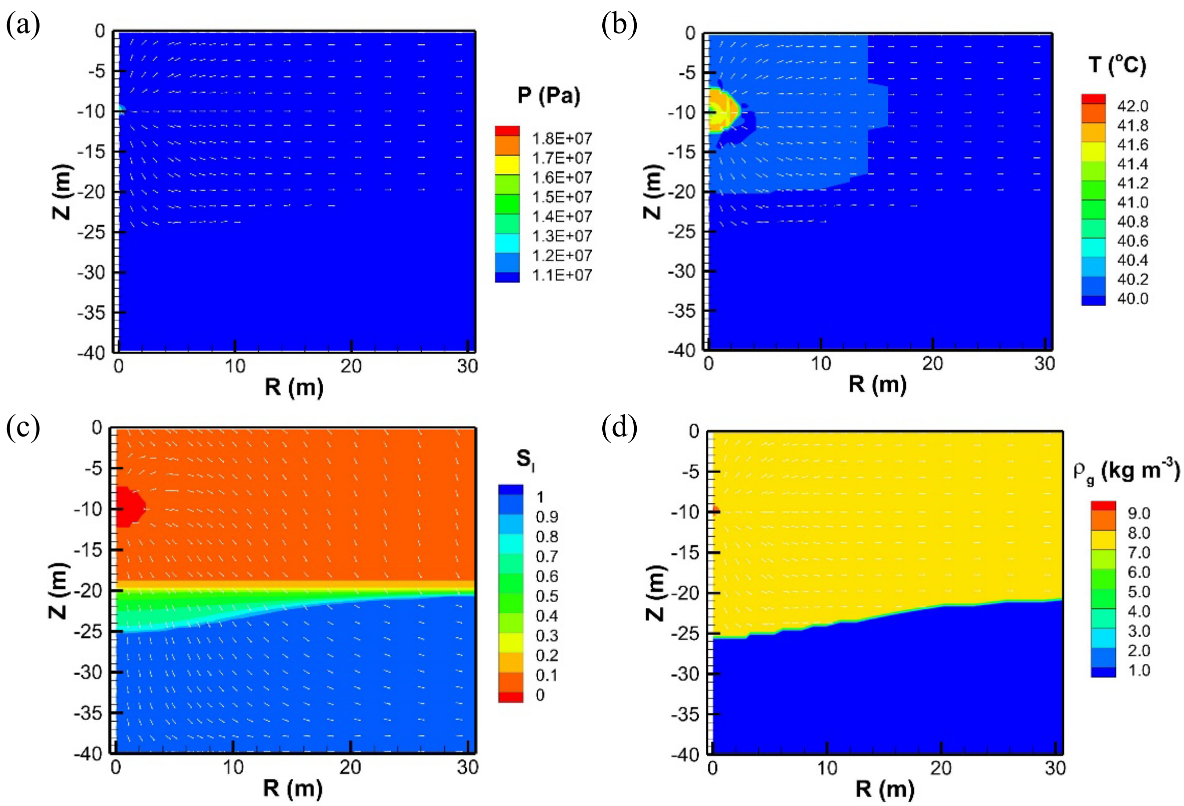

Figure 9. Simulation results for the subregion (0 m < R < 30 m) for the case of injection of H_2 at 5.5 kg/s at t = 6 hrs showing (a) pressure and gas velocity direction vectors, (b) temperature and gas velocity-direction vectors; (c) liquid saturation (S_l) and liquid velocity-direction vectors; and (d) gas density.

Figure 10 shows the simulation results after six hours of withdrawal. Note the minor decompression-related heating below the withdrawal blocks at R = 0, Z = -40 m due to the negative Joule-Thomson coefficient of H_2. The main result to note in Figure 10 is the recovery of the gas-water interface from its downconed position after six hours of injection to its recovered position after six hours of withdrawal. The simulation shows that injection causes a downconing (pushdown) effect on the gas-water interface that reduces the height of upconing relative to the well bottom location during the subsequent withdrawal period. It appears that this daily cyclic six-hour I/W use case mitigates the detrimental effects of upconing. In short, injection depresses the gas-water interface, and withdrawal tends to restore it to its initial position rather than pulling it up to the bottom of the well.

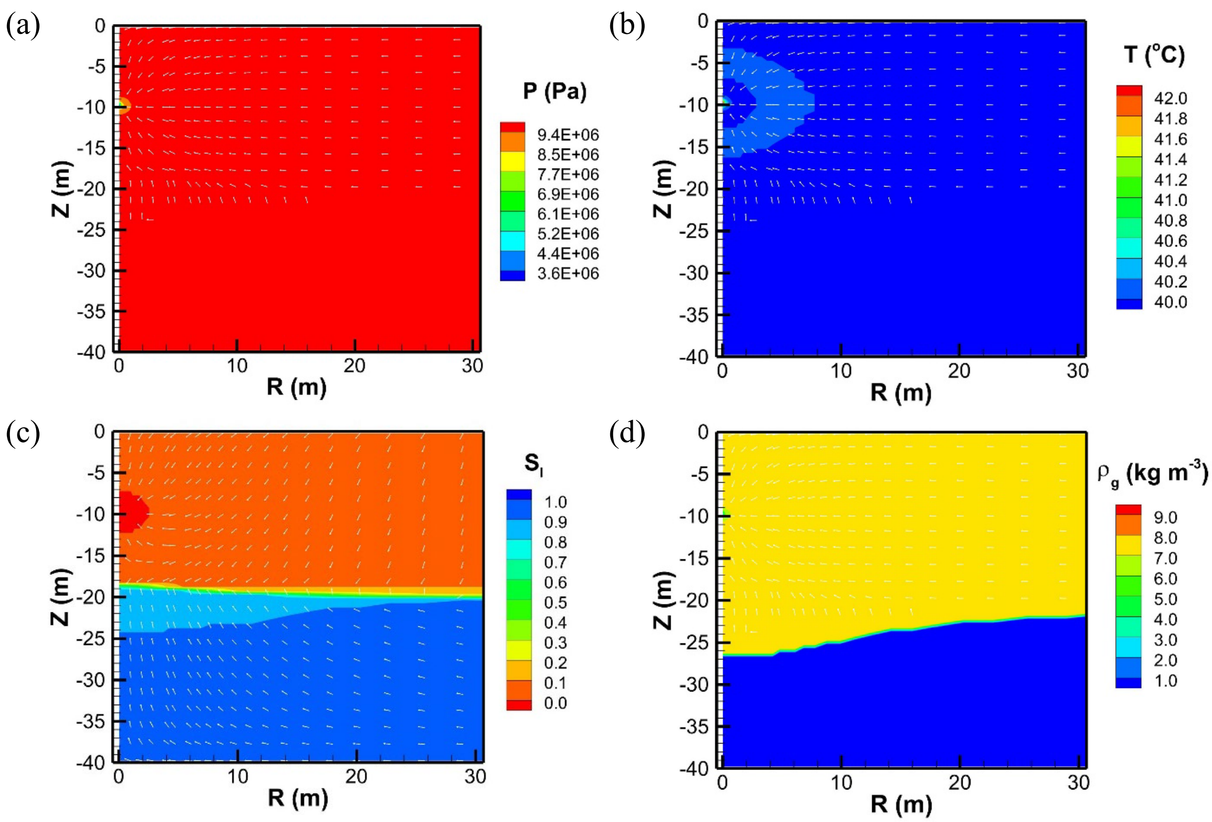

Figure 10. Simulation results after 6 hrs of withdrawal of H_2 (total t = 12 hrs) in the subregion 0 m < R < 30 m showing (a) pressure and gas velocity direction vectors, (b) temperature and gas velocity direction vectors; (c) liquid saturation (S_l) and liquid velocity direction vectors; and (d) gas density.

Figure 11 shows results following the 12 hours of shut-in associated with the use case (total *t* = 24 hrs). Frame (c) shows the continued recovery of the gas-water interface to its initial horizontal position. Overall, despite the interesting thermal effects observed (e.g., Figure 9b), we conclude that the magnitude of the effects is very small, and non-isothermal effects are not important for analyzing the issue of upconing as a detriment to technical feasibility of UHS.

The simulation results of the cyclic use case involving a mass-balanced six hours of injection and withdrawal shown in Figures 9–11 show that cycling tends to mitigate upconing of water toward the well because injection causes downconing or depression of the gas-water interface, while withdrawal causes the gas-water interface to move back upwards. But because the gas-water interface starts in a downconed position for withdrawal, it tends to be pulled upward only close to its starting (horizontal) position rather that up to the well as it tends to do when starting withdrawal with a horizontal gas-water interface. In order to evaluate this effect more fully, we carried out multiple cycles of I/W and observed a net upconing effect as described below in Section 7.2.

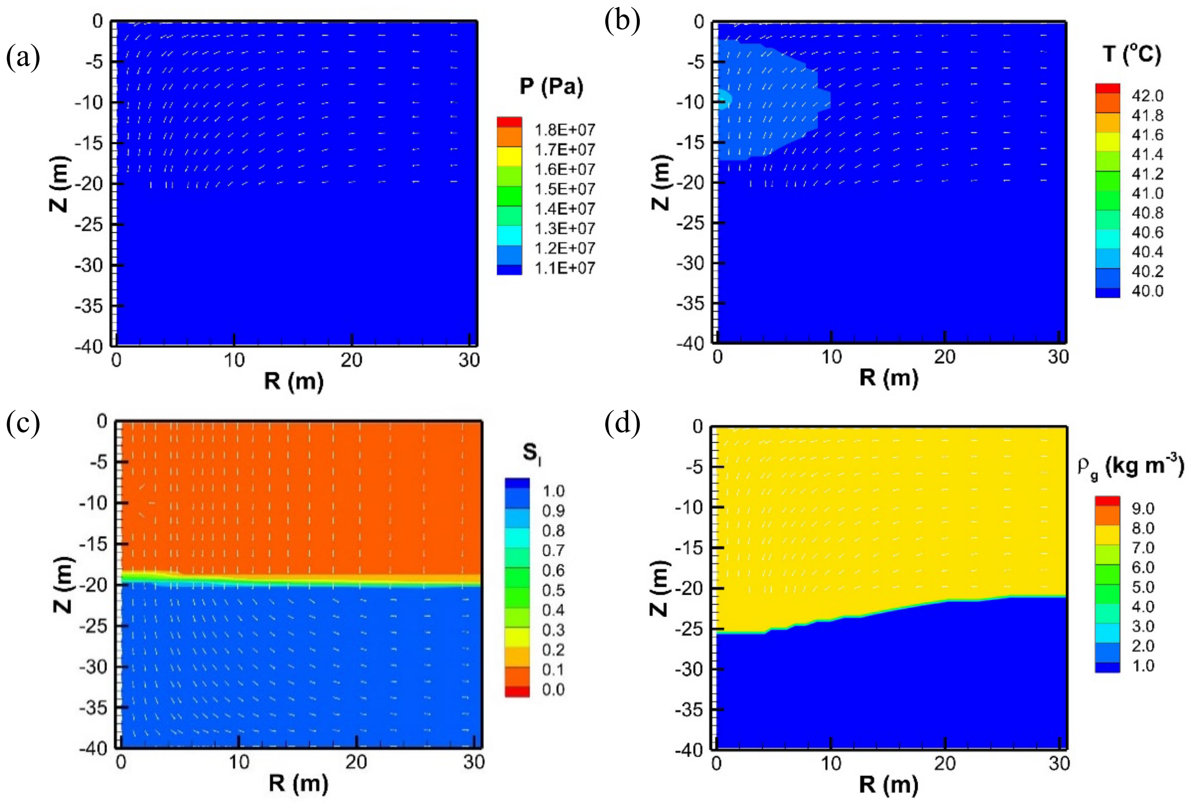

Figure 11. Simulation results after 12 hours of shut-in (total t = 24 hrs) showing (a) pressure and gas velocity direction vectors, (b) temperature and gas velocity vectors; (c) liquid saturation (S_l) and liquid velocity vectors; and (d) gas density.

7 Sensitivity Analysis of Water Upconing

7.1 DB Model Sensitivity Analysis

Although the DB model results presented in a previous section were shown to be very approximate for water upconing in UHS, the DB model was shown to account for fundamental controls on upconing and is therefore useful for sensitivity analyses. Using the Argo add-in to Excel, Monte Carlo simulations of the DB model were carried out followed by a sensitivity (correlation) analysis. Pearson sensitivity coefficients based on 1000 trials using random samples from uniform distributions as shown in Table 4 are reported in Tables 5–7. We color-coded the influence of the top three parameters from highest (red), intermediate (green), to lowest (blue).

As shown, k_H is consistently the most important parameter controlling upconing, with high k_H favoring less upconing. K_V is also important, but much less so than k_H. The reason for this is that high k_H allows lateral flow from the large and laterally expanding radial volume to the well, preventing the hydraulic drawdown that leads to upconing. High k_V has the same effect of preventing drawdown, but the reservoir volume available to provide fluid vertically to the well is miniscule compared to the access to reservoir volume facilitated by k_H.

The sensitivity analysis shows the expected large influence of porosity (ϕ) at early times, and decline in importance at late times. Regarding the engineered (operational) parameter, withdrawal rate (Q), the sensitivity analysis shows Q not being all that influential. Note that this is partly a result of different scaling factors applied to different parameters (Finsterle, 2015). The sampling range for the natural, highly variable or uncertain permeabilities is considerably larger than the range over which the human-controlled operational parameter (specifically Q) are varied. Moreover, permeability varies by orders of magnitude (we therefore sample it in logarithmic space), making it appear very influential because "small" changes in k are actually quite large in absolute terms. On the other hand, Q varies only by 50%. This points out that one needs to characterize permeability very carefully to reduce uncertainty in k, making predictions of upconing more accurate and allowing for a more reliable optimization of operational choices (e.g., Q, d, properties and density of wells, etc.). The initial distance of the well from the interface (d) is also quite important and should be chosen as large as possible to mitigate upconing.

Table 4. Distributions for the 1000-trial Monte Carlo sensitivity analysis of the DB model.

	Log k_H (log m^2)	Log k_V (log m^2)	Porosity ϕ	Q (m^3 s^{-1})	d (m)
Uniform Distribution	(-13, -11)	(-13, -11)	(0.08, 0.22)	(0.6, 0.9)	(5, 15)

*Table 5. Pearson sensitivity coefficients for water upconing during H_2 withdrawal for DB model at a radius of 0.01 m (i.e., at the well) with the top three most influential variables for short and long times color coded by decreasing influence from red-green-blue (***-**-*).*

Time Period	k_H	k_V	ϕ	Q	d
Short 100 s	0.468***	0.413**	0.070	0.087	0.250*
Long 6 hrs	0.760***	0.132*	0.04	0.106	0.268**

*Table 6. Pearson sensitivity coefficients for water upconing during H_2 withdrawal for DB model at a radius of 10 m with the top three most influential variables for short and long times color coded by decreasing influence from red-green-blue (***-**-*).*

Time Period	k_H	k_V	ϕ	Q	d
Short 100 s	0.286**	0.274*	0.500***	0.189	0.080
Long 6 hrs	0.826***	0.224**	0.174*	0.109	0.158

*Table 7. Pearson sensitivity coefficients for water upconing during H_2 withdrawal for DB model at a radius of 20 m with the top three most influential variables for short and long times color coded by decreasing influence from red-green-blue (***-**-*).*

Time Period	k_H	k_V	ϕ	Q	d
Short 100 s	0.190*	0.102	0.588***	0.249**	0.071
Long 6 hrs	0.814***	0.329**	0.196	0.178	0.152*

Note in Tables 5–7 the increasing influence of k_V on upconing at $t = 6$ hrs as r increases from 0.01 to 10 to 20 m (Pearson coefficients 0.132, 0.224, 0.329, respectively). To better illustrate the sensitivity results, we can show explicitly the control of k_V on cone radius in the DB model by holding k_H constant at 1 Darcy (10^{-12} m^2) and varying k_V from 0.1 to 10 Darcies (10^{-13} to 10^{-11} m^2). The profiles of upconing calculated by the DB model for these variations are shown in Figure 12 at 600 hours (near steady state). As shown, the steady-state upconing distance is the same for the three different values of k_V, but the size (radius) of the upconed region is significantly larger for the smaller values of k_V.

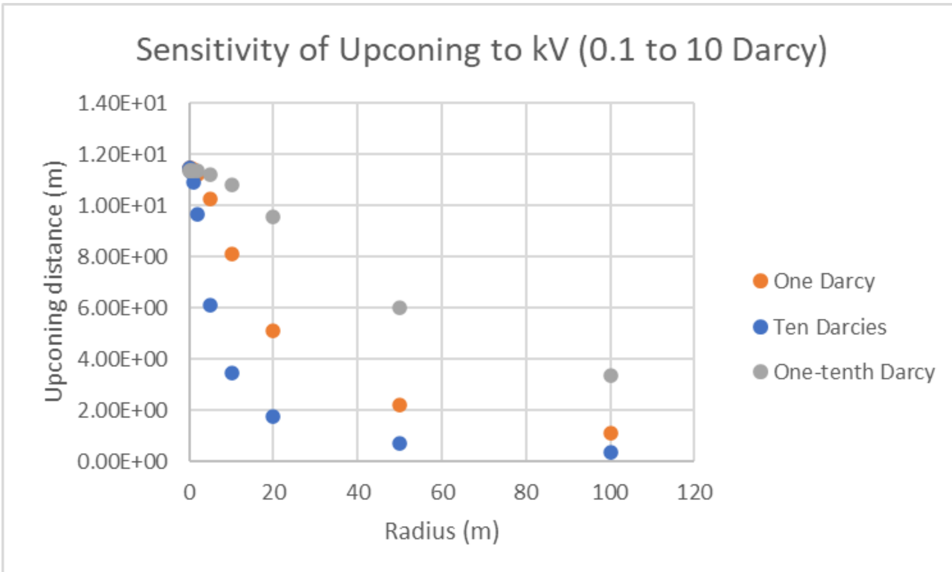

Figure 12. Upconing profiles for three different values of k_V and constant k_H (10^{-12} m^2) showing the broadening of the upconed region that occurs for smaller k_V.

7.2 Sampling-Based Sensitivity Analysis using Multi-Cycle Model

In the previous subsections, the degree of upconing and the factors affecting it were examined for systems with increasing complexity. Moreover, the I/W well was modeled roughly as a point sink or source to match the assumption of the DB model. Only one withdrawal period or a single I/W cycle was considered, and capillary pressures were ignored. In this final sensitivity analysis, some of these simplifying assumptions are removed to include additional aspects representative of the use case with daily I/W cycles for the storage of green hydrogen, as described in Section 4.2. Despite the added realism, the model remains generic; additional complexities can be added once information about site-specific formation characteristics and the operational design become available.

In this model of upconing, we again look at a radial system of the storage reservoir at a depth of approximately 1 km, where a 20 m thick gas cap has been emplaced within the storage aquifer prior to the beginning of cyclic I/W operations. The well is considered to be perforated starting from the top of the storage formation towards the gas-water interface. The length of the perforated well section is 10 m for the base case, but will be varied as part of the sensitivity analysis. The magnitude of the injection and withdrawal rates are identical, with the sink and source terms specified at the top of the perforated well interval. As before, a daily cycle consists of six hours of H_2 injection, six hours of gas withdrawal, and 12 hours of shut-in (see schedule shown in Figure 3); 100 such cycles are simulated. The domain dimensions and boundary conditions as shown in Figure 4. Reference properties are as shown in Table 3 except we include capillary pressure using van Genuchten's water retention function (Luckner et al., 1989) with a capillary strength parameter α of 0.001 Pa^{-1}.

Figure 13 shows the movement of the gas-water interface over time immediately below the well relative to its initial elevation at -20 m below the caprock. Negative values indicate downconing, i.e., the depression of the saturated zone due to the high gas pressures caused by hydrogen injection. Positive values reflect upconing of the gas-water interface towards the well during withdrawal. The upconing here amounts to less than 5 m; consequently, there is no water breakthrough to the well (watering out).

Note that gas-water interfaces in porous media are not sharp under the conceptualization of two-phase flow in porous media by Darcy's law. Particularly during the hydrogen injection period, capillary forces and flow interference between the advancing gas and regressing liquid phases create a relatively broad region with both phases present at intermediate saturations. However, even under static conditions, capillary forces lead to a fringe zone with a transitional saturation profile that follows the prescribed water retention curve. In what follows, the location of the gas-water interface is defined as a saturation-weighted distance, which very closely reflects the height of the gas-water interface during the withdrawal period (i.e., capturing the relevant upconing distance); during downconing, the same saturation-weighted distance is an approximate distance of how far the gas plume penetrates into the groundwater.

As shown in Figure 13, during the first injection of hydrogen, the initially flat gas-water interface is depressed by approximately 2.3 m at the center of the radial system (under the well). Upconing during the subsequent withdrawal period reverses that process and leads to an additional upconing of about 1.3 m above the elevation of the initial gas-water interface. Despite using the same injection and withdrawal rates, the relative upconing distance (approximately 3.6 m) is greater than the first downconing distance (2.3 m). This asymmetry reflects a stronger pressure drop during withdrawal relative to pressure drop during injection. One reason for the larger pressure drop during withdrawal is that the volumetric gas flux during withdrawal at constant mass flow rate is larger than during injection when the gas is compressed.

During the 12-hour shut-in period, the weak radial pressure gradient of the small water mound leads to a slow recovery and thus minor gas-water interface decline. As a result, at the beginning of the second cycle, the gas-water interface is slightly elevated above its initial depth. During the second and subsequent gas injections, it is increasingly easier to displace the fluid of the elevated water cone compared to the flat initial condition, as water in the upconed region is closer to the injection well. Moreover, there already exists a radial pressure gradient supporting the lateral and downward water displacement. This leads to a somewhat greater relative drop in the gas-water interface, albeit from an ever-rising elevation of the starting point at the end of each shut-in period. With each cycle, the gas-water interface is raised. This super-elevation is asymptotic as upconing is countered by the increasing weight of the water mound, a faster recovery during the shut-in period, and a more efficient downconing during injection. After about 30 daily cycles, the maximum upconed interface elevation is essentially stabilized at a value of 4.8 m above its initial elevation. The amplitude of the gas-water interface fluctuations increases from 3.6 m for the first cycle to approximately 4.2 m. This evolution indicates that the asymmetry of downconing and upconing during the injection and withdrawal periods, respectively, requires that the dynamics of repeated cycling must be taken into account for the estimation of maximum upconing. However, a near-steady value is reached after about 30 days, a very short spin-up period relative to the intended duration of a hydrogen storage project.

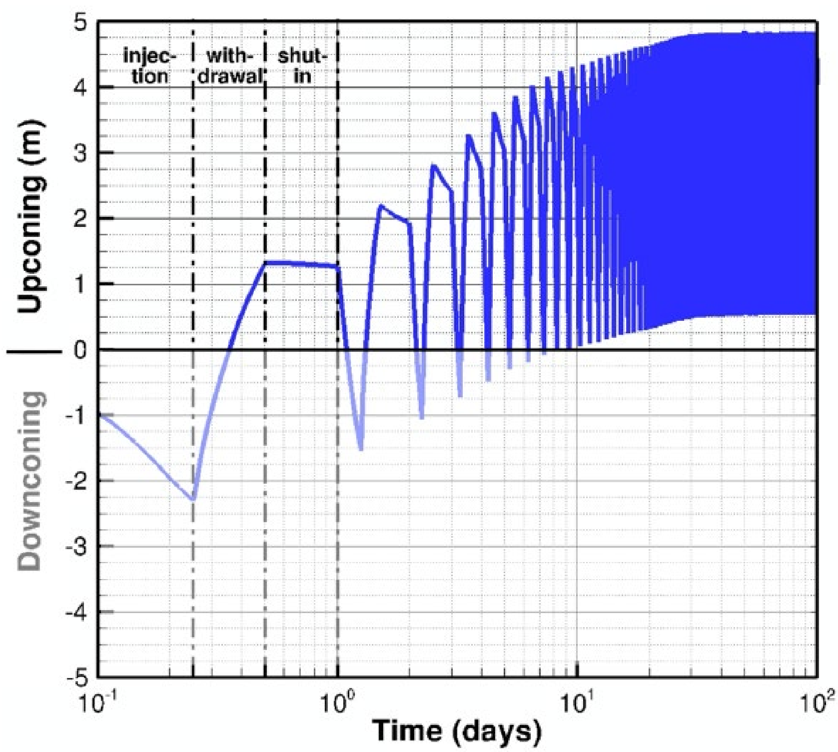

Figure 13. Saturation-weighted downconing and upconing distances relative to the initial elevation of the gas-water interface at -20 m below the caprock as a function of time.

Figure 14 shows the saturation distributions at the end of the first and last injection and withdrawal cycle, indicating the broader and widening saturation fronts during downconing, whereas the fringe zone during upconing remains narrow and constant. Maximum upconing after the first withdrawal is limited (1.3 m above the initial gas-water interface), but is considerably higher (4.8 m) and radially more extensive once the system is stabilized. These results are for non-hysteretic k_{rel}, and may look different if hysteretic k_{rel} is modeled (e.g., Bo et al., 2023).

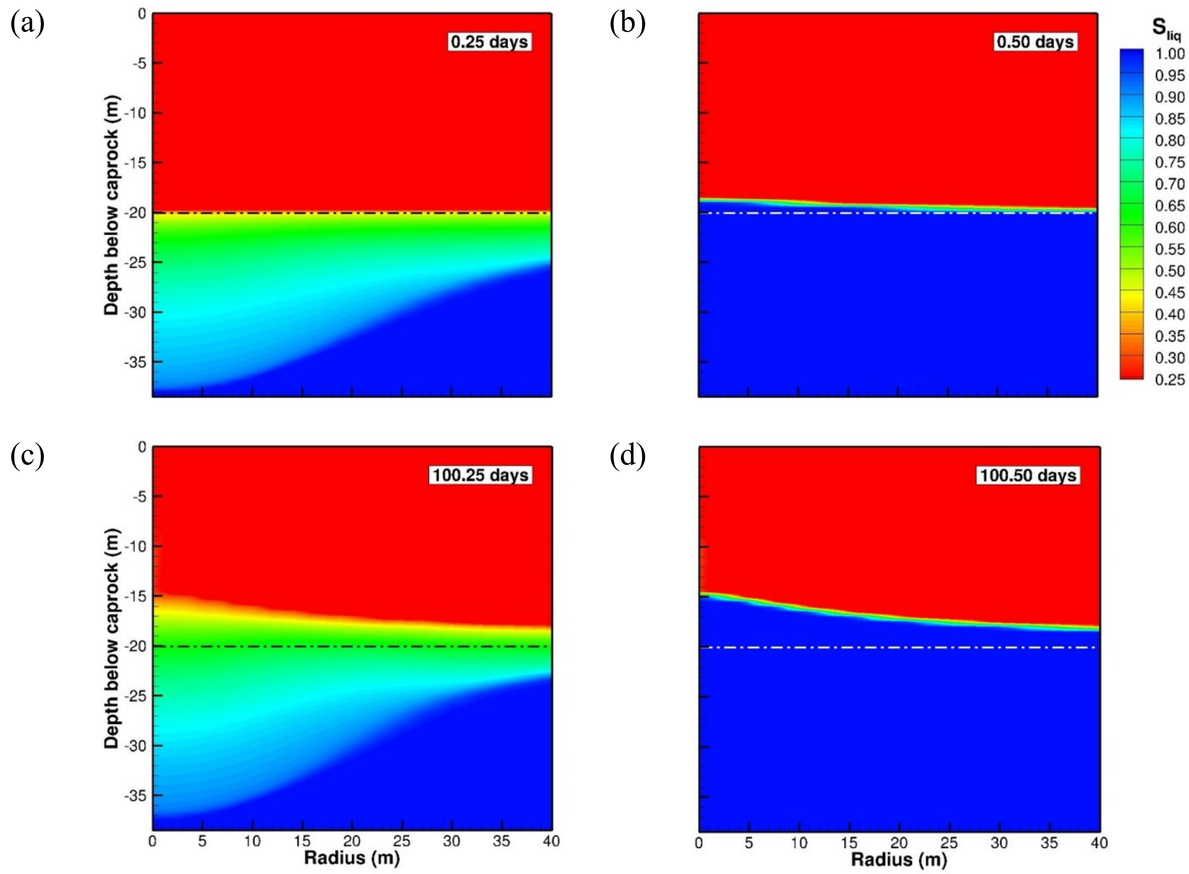

Figure 14. Saturation distributions showing downconing after hydrogen injection at (a) 0.25 days and (c) 100.25 days, and upconing after gas withdrawal at (b) 0.5 days and (d) 100.5 days, i.e., after one and 101 daily cycles.

Using the model described above, we present next a sampling-based, global sensitivity analysis in which previously discussed key parameters of upconing are varied. Each model input parameter is independently and randomly sampled (using Latin hypercube sampling) from a uniform distribution over the ranges indicated in Table 8. The samples are then randomly combined into 300 parameter sets. For a sensitivity analysis, the purpose of sampling is simply to explore the parameter space, which calls for the use of a uniform distribution that avoids correlations among the parameters. (This is different from the sampling design used for uncertainty quantification, where typically a non-uniform, distribution is selected to reflect the uncertainty or variability of the input parameters, and where correlations among the parameters are to be accounted for.)

Table 8. Ranges of parameters uniformly sampled for a global sensitivity analysis.

Parameter	Minimum value	Maximum value
Injection / withdrawal rate (kg/s)	0.0	10.0
Distance of well bottom to gas-water interface (m)	0.0	15.0
$\log_{10}$[horizontal permeability (m^2)]	-12.0	-10.0
$\log_{10}$[vertical permeability (m^2)]	-12.0	-10.0
porosity	0.05	0.20

Figure 15 shows the 300 samples of the I/W rate as an example. The red regression line is horizontal and passes through the midpoint of the parameter range, demonstrating that the sampling is unbiased. The cross-plot of the sampled rate and horizontal permeabilities covers the desired parameter space. The red regression line is horizontal, confirming that the sampled parameters are not correlated to each other.

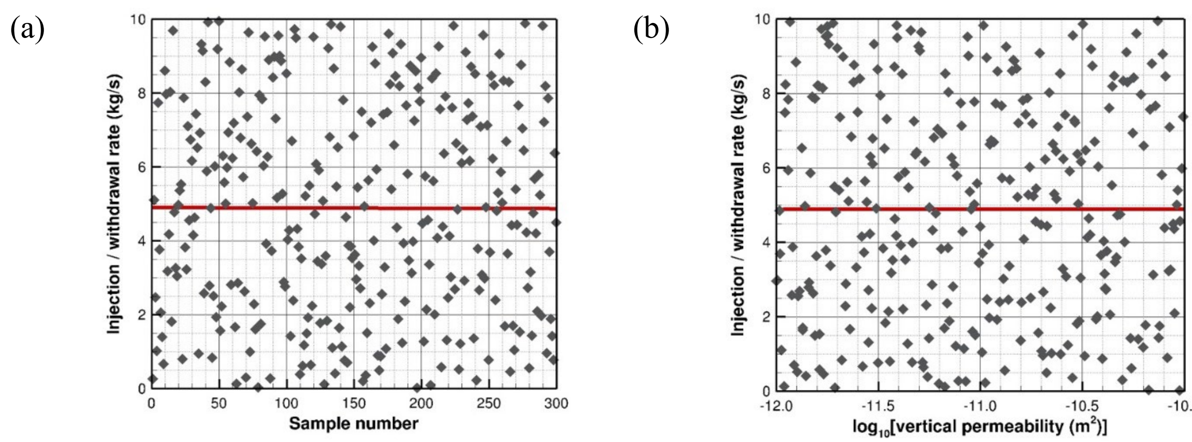

Figure 15. Example of random sampling of input parameters: The horizontal regression lines indicate (a) that sampling is uniform and (b) uncorrelated.

For each of the 300 parameter sets, the model is run for 10 days, simulating 10 cycles of hydrogen injection, gas withdrawal, and shut-in recovery, approaching the stabilized value of the long-term upconing maximum. While the entire system state at any point in space and time is available for each of the 300 realizations, we focus here on a single performance metric of interest, which is the maximum upconing distance from the initial gas-water interface towards the well at the end of the withdrawal period.

Figure 16 shows the calculated upconing distance for each realization. The uniformly sampled and randomly combined input parameter sets yield a non-uniform, skewed distribution of upconing distances.

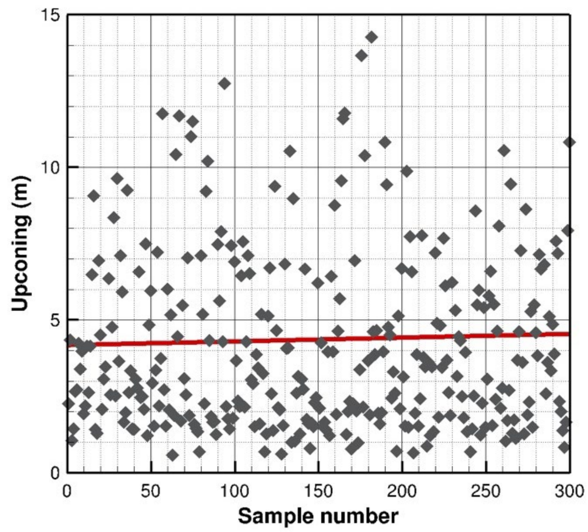

Figure 16. Maximum upconing distance simulated for 300 random, uncorrelated parameter sets.

Multiple global sensitivity analysis methods exists that provide composite, statistical measures that show the relative influence of parameters and the degree model to which predictions are affected by non-linearities and parameter interactions (Saltelli et al., 2008; Wainwright et al., 2014). Here, we simply provide the scatter plots as a direct visual means for identifying the relative influence of a parameter on the predicted upconing distance.

Each panel of Figure 17 contains the same scatter points of upconing as those shown in Figure 16. However, they are rearranged to reveal their dependence on each of the five model input parameters. For a given parameter value on the horizontal axis, the vertical scatter indicates the variability obtained by randomly changing the other four adjustable parameters.

The regression line shows the average dependence of upconing with respect to the selected parameter. A horizontal regression line indicates that the corresponding parameter has no influence on upconing; a steeply sloping regression line indicates that the parameter is influential, as the systematic impact of changing the parameter is significant compared to the variability in upconing caused by randomly changing the other parameters. The positive or negative slope indicates the sign of the sensitivity coefficient. Because the performance metric (vertical axis) is the same for all plots, and the ranges given in Table 8 can be considered reasonable as they reflect the expected variability of storage formation properties (permeabilities and porosity) and design parameters (rate and well penetration), the slopes can be directly compared to each other as a measure of relative parameter influence.

Based on such a comparison of the slopes of the regression lines, the horizontal permeability is identified as the parameter with the greatest influence on upconing, consistent with the findings previously presented in Section 7.1. The negative slope reveals that the higher the horizontal permeability, the smaller the water upconing in response to gas withdrawal. Note that the scatter plot suggests that the slope of the average upconing changes with permeability, with higher sensitivities for low permeability values and lower sensitivities for high permeabilities. This is expected due to the physical limit of zero upconing at very large permeabilities. While the linear regression does not capture this non-linearity, its purpose of representing an average influence of the selected parameter range is preserved, and the full sensitivity structure is revealed by the scatter plot. It also demonstrates that a local sensitivity analysis, which assumes that sensitivities do not change over the parameter range of interest, may not be appropriate.

The vertical permeability (Figure 17d) is also an influential parameter, but less so than the horizontal permeability (Figure 17c) and the pumping rate (Figure 17a). As discussed above, increasing vertical permeability increases upconing (as indicated by the positive slope of the regression line), which is opposite to the impact that horizontal permeability has on upconing.

As expected, the gas withdrawal rate is an important design parameter that can be used to control and mitigate potential upconing issues, e.g., by adjusting well-specific withdrawal rates, or installing additional wells. Well penetration, however, has a weaker influence. While a deeper well gets closer to the gas-water interface—potentially leading to water intake at the bottom of the well—the pressure drawdown is reduced because gas can be withdrawn over a longer perforated well section. The second aspect appears to dominate the system behavior, leading to a positive slope of the regression line with increasing upconing for shorter production intervals despite the fact that the well ends farther away from the initial gas-water interface. (Note that this more realistic conceptualization of a UHS well is not present in the DB model, which conceptualized the well as a point source/sink at a distance *d* from the initial gas-water interface.) While water may be drawn into the well, it is likely to remain near the bottom of the well rather than being lifted to the land surface as gas enters more and more from the upper perforations of the well if the lower part fills with water. The simulations show that most of the gas is produced from the top of the storage reservoir near the caprock. Finally, the porosity has only a minor impact on the stabilized upconing distance, as discussed in Section 7.1.

The scatter plots enable a global sensitivity analysis in a five-dimensional parametric hypercube. Figure 17f shows a three-dimensional representation of the joint impact of the two most influential parameters—withdrawal rate and horizontal permeability—on water upconing, which is shown on the third, vertical axis. As before, it shows that the largest upconing is experienced in formations with relatively low horizontal permeability (i.e., at the back side of the cube) and that upconing increases from left to right as withdrawal rates are increased. Not surprisingly, the realization leading to the largest upconing (Sample 183, see Figure 16) has its values at the bounds of a pair of highly influential reservoir parameters, i.e., a horizontal permeability of 10^{-12} m^2 (see Figure 17c) and a vertical permeability of 10^{-10} m^2 (see Figure 17d). A somewhat stronger upconing would be achieved if the withdrawal rate were at its maximum of 10 kg/s rather than at the sample-point value of 4.4 kg/s (Figure 17a).

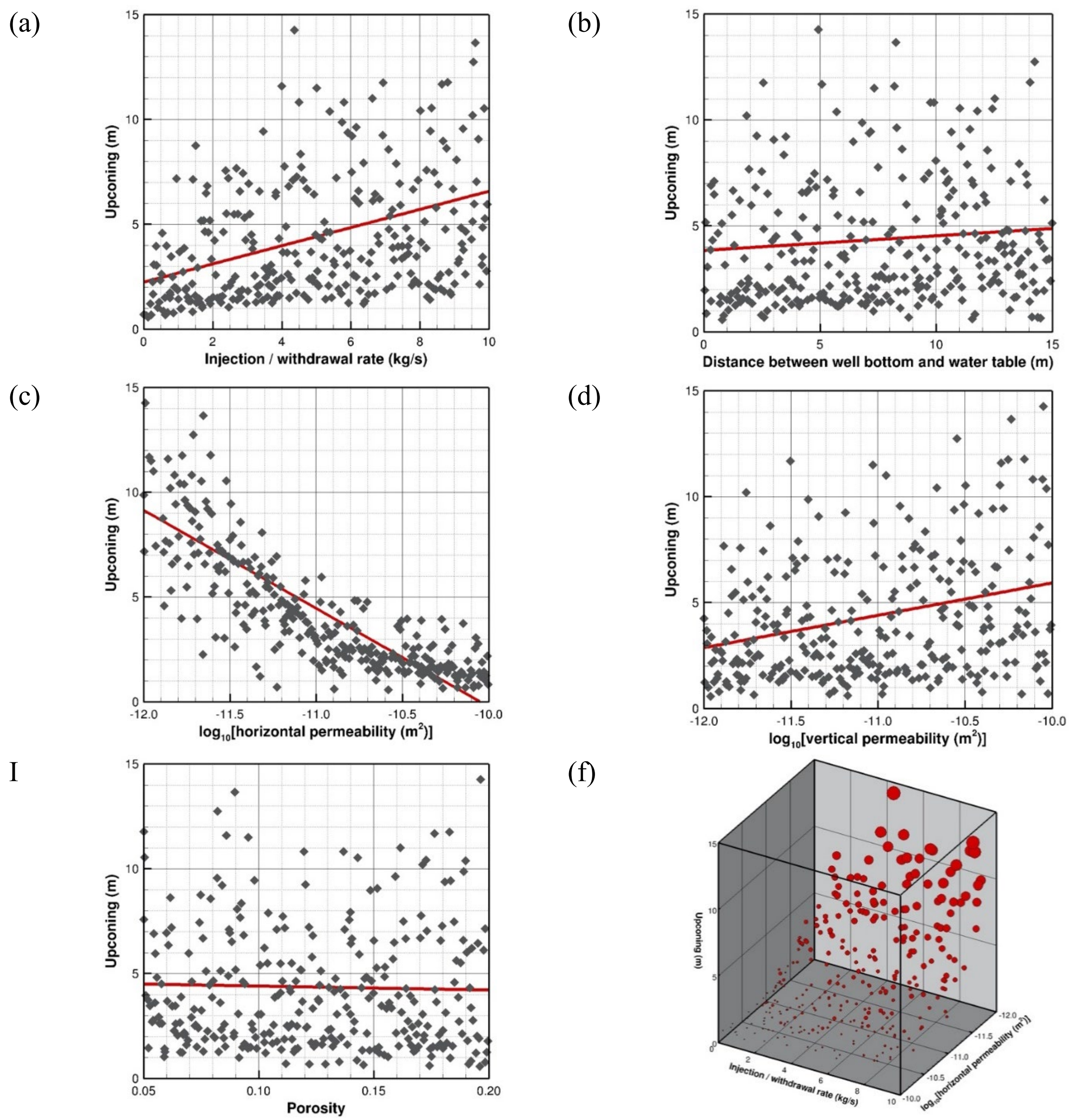

Figure 17. Maximum upconing distance after 10 cycles as a function of (a) pumping rate, (b) well penetration, (c) horizontal permeability, (d) vertical permeabilitI(e) porosity, and (f) rate and horizontal permeability; slopes of regression lines indicate parameter influence.

8 Implications for UHS Design and Operation

In this study, we carried out modeling and simulation of water upconing to answer two basic questions relevant to UHS:

1. Under what reservoir and operating conditions is upconing a potential problem for UHS?

2. What is the relative importance of the various reservoir properties and operating conditions for water upconing?

Addressing Question 1, this study shows that reservoirs with low k_H are the most susceptible to upconing. The vertical permeability (k_V) is also important in controlling upconing height, but much less so than k_H. Reservoirs with low k_V can be expected to have a broader diameter of the upconed water, and upconing may be slower, i.e., longer withdrawal periods are possible without upconed water entering the well. High porosity (ϕ) disfavors upconing because there is less pressure drawdown due to withdrawal when there is more pore space filled with compressible gas. At very short times, porosity is very influential, but for practical purposes of assessing potential impact of water reaching the well, the porosity is not a significant property. In addition, porosity does not vary all that much across and within good quality storage reservoirs.

On the operational side, i.e., regarding factors of the system that can be designed and engineered by operators, large withdrawal rate and small distance from well to gas-water interface are obvious contributors to water upconing into the well. If there is a gas-water interface in the reservoir, operators should design wells with withdrawal perforations/screens as far from the gas-water interface as possible, and withdrawal rates should be as low as possible. Individual well withdrawal rates can potentially be reduced by installing additional wells while maintaining constant reservoir-wide I/W rate. Cyclic I/W schedules with roughly balanced flow rates are favorable for reducing upconing to wells, specifically at the beginning of the operation.

Regarding Question 2, this study showed by sensitivity analyses using both the analytical DB model and fully coupled two-phase numerical simulation that k_H is the most important property of the system controlling upconing of water at short and long periods, both close to and far from the well. Vertical permeability is generally the second most important property controlling upconing, particularly at long times. Distance from bottom of well to gas-water interface (d) and the withdrawal rate (Q) are important and must be properly engineered to avoid upconing. Porosity is also an important property, but only over short periods of withdrawal.

The constraints imposed by the simplifying assumptions of the DB model can be removed by using numerical models with more realism and carrying out multi-cycle simulations and sensitivity analyses with these models. For example, use of a more realistic well conceptualization and inclusion of capillary pressure in the study provided detailed results of the dynamics and irreversibility of upconing and downconing, albeit for a generic single-well system. The simple scatter plots provide a practical tool for the calculation of transparent sensitivity and performance measures. Moreover, such plots could be used to develop acceptance criteria for potential storage sites and to design the storage system in terms of well properties, perforation locations, I/W rates, etc. From a performance risk perspective, one could weigh each scatter point by the input parameter's site-specific uncertainty distribution and then determine the acceptable range of the controllable operational parameters for a selected risk tolerance.

9 Conclusions

We have carried out a study on water upconing in UHS. We pointed out that any analysis of UHS needs to start with a precise definition of the use case so that important parameters related to upconing (I/W schedule and rate) can be defined and investigated. The relatively simple DB model and the fully coupled simulator iTOUGH2-EOS7CH were used to estimate upconing and downconing distances and dynamics, and to carry out sensitivity analyses to determine the controls on upconing so that it can be mitigated. Our analyses showed that the simple DB model agrees generally with numerical simulations for both its intended purpose (i.e., single-phase water-brine upconing) and it can be used for rough estimates of upconing in the two-phase system H_2-water. Nevertheless, two-phase multicomponent systems involve many mechanisms and details that require a reservoir simulator. The mechanistic simulation of these coupled processes are essential to applications involving more realistic and heterogeneous systems in practice over multiple cycles of I/W, e.g., for aquifer storage (e.g., Pfeiffer and Bauer, 2019) and those involving gas mixtures in depleted natural gas reservoirs (e.g., Lysyy et al., 2021).

The main effect of multiple I/W cycles involving short periods of balanced mass-based I/W, such as the six-hour cycle use case studied here, is the net upconing that occurs following withdrawal. In short, the push-down of the gas-water interface during injection helps mitigate upconing during withdrawal, but it is not exactly balanced, leading to a slight rise in the gas-water interface relative to the initial flat interface following each withdrawal. This net upconing stabilizes after a few tens of days (cycles) in the system studied here.

Sampling-based global sensitivity analysis of multiple cycles of simulated UHS confirmed that horizontal permeability is the main factor controlling upconing. The analysis also showed that horizontal permeability is a stronger control on upconing when permeability is low and less sensitive when permeability is high. The vertical permeability is also an influential parameter, but less so than the horizontal permeability. Gas withdrawal rate is an important design parameter that can be used to control and mitigate potential upconing issues. Well penetration, however, was shown to have a weaker influence. In practice, results of sensitivity analyses could be used to develop acceptance criteria of the various intrinsic properties and operational (use case) parameters for evaluation and design of potential storage sites.

10 Acknowledgments

This work was supported by a grant from EPRI to Finsterle GeoConsulting LLC.

11 Nomenclature

Symbols	Description	Units
d	Distance for original gas-water interface to well bottom	m
D	Molecular diffusivity	$m^2\ s^{-1}$
k_H, k_x, k_r	Permeability in the horizontal direction	m^2
k_V, k_Z	Permeability in the vertical direction	m^2
K_H	Hydraulic conductivity in the horizontal direction	$m\ s^{-1}$
K_V	Hydraulic conductivity in the vertical direction	$m\ s^{-1}$
P	Pressure	Pa, bar
Q	Volumetric I/W rate	$m^3\ s^{-1}$
Q_m	Mass-based I/W rate	$kg\ s^{-1}$
R	Radial coordinate	m
R'	Intermediate term in DB model	-
S	Phase saturation (S_l = aqueous, S_g = gas)	-
T	Temperature	°C
X	Mass fraction	-
Z	Vertical coordinate	m
Greek Symbols		
ϕ	Porosity	-
γ	Gas density in DB model	$kg\ m^{-3}$
γ'	Intermediate term in DB model	$m\ s^{-1}$

12 References

Arthur, J.D., Alleman, N. and Andersen, K., 2016. A Historical Look at Underground Natural Gas Storage in America, *Oil-Industry History*, 17(1), pp. 35-46. Accessed May 1, 2023.

https://archives.datapages.com/data/phi/v17-2016/arthur-alleman-andersen.htm

Bell, I.H., Wronski, J., Quoilin, S. and Lemort, V., 2014. Pure and pseudo-pure fluid thermophysical property evaluation and the open-source thermophysical property library CoolProp. *Industrial & engineering chemistry research*, *53*(6), pp.2498-2508.

Bo, Z., Boon, M., Hajibeygi, H. and Hurter, S., 2023. Impact of experimentally measured relative permeability hysteresis on reservoir-scale performance of underground hydrogen storage (UHS). *International Journal of Hydrogen Energy*, *48*(36), pp.13527-13542.

Booze-Allen, Argo add-in for Excel, accessed April 30, 2023

https://boozallen.github.io/argo/

CalISO, accessed April 30, 2023.

http://www.caiso.com/informed/Pages/ManagingOversupply.aspx

Blain, Loz, 2022. Record-breaking hydrogen electrolyzer claims 95% efficiency, NewAtlas, accessed April 30, 2023

https://newatlas.com/energy/hysata-efficient-hydrogen-electrolysis/

Chandler, R.L. and McWhorter, D.B., 1975. Upconing of the salt-water–fresh-water interface beneath a pumping well. *Groundwater*, *13*(4), pp.354-359.

Dagan, G. and Bear, J., 1968. Solving the problem of local interface upconing in a coastal aquifer by the method of small perturbations. *Journal of hydraulic research*, *6*(1), pp.15-44.

Falcone, G. and Barbosa Jr, J.R., 2013. State-of-the-art review of liquid loading in gas wells. DGMK/ÖGEW-Frühjahrstagung 2013, Fachbereich Aufsuchung und Gewinnung Celle, 18./19. Accessed July 13, 2023. https://www.osti.gov/etdeweb/servlets/purl/22124955

Finsterle, S., M. Commer, J. Edmiston, Y. Jung, M.B. Kowalsky, G.S.H. Pau, H. Wainwright, and Y. Zhang (2017). iTOUGH2: A Multiphysics simulation-optimization framework for analyzing subsurface systems. *Computers and Geosciences*, *108*, 8–20, doi:10.1016/j.cageo.2016.09.005.

Finsterle, S. (2022), Enhancements to the TOUGH2 Simulator Implemented in iTOUGH2. Report FGC-18-02/LBNL-7016E, Finsterle GeoConsulting, LLC, Kensington, Calif.

Finsterle, S., 2015. Practical notes on local data-worth analysis. *Water Resources Research*, *51*(12), pp.9904-9924.

Foh, S.; Novil, M.; Rockar, E.; Randolph, P. Underground hydrogen storage. final report. [salt caverns, excavated caverns, aquifers and depleted fields]; Brookhaven National Lab.: Upton, NYUSA, 1979.

Heinemann, N., Alcalde, J., Miocic, J.M., Hangx, S.J., Kallmeyer, J., Ostertag-Henning, C., Hassanpouryouzband, A., Thaysen, E.M., Strobel, G.J., Schmidt-Hattenberger, C. and Edlmann, K., 2021. Enabling large-scale hydrogen storage in porous media–the scientific challenges. *Energy & Environmental Science*, *14*(2), pp.853-864.

Jangda, Z., Menke, H., Busch, A., Geiger, S., Bultreys, T., Lewis, H. and Singh, K., 2023. Pore-scale visualization of hydrogen storage in a sandstone at subsurface pressure and temperature conditions: Trapping, dissolution and wettability. *Journal of Colloid and Interface Science*, *629*, pp.316-325.

Johns, R.T., Lake, L.W., Ansari, R.Z. and Delliste, A.M., 2005. Prediction of capillary fluid interfaces during gas or water coning in vertical wells. *SPE Journal*, *10*(04), pp.440-448.

Katz, D.L. and Tek, M.R., 1981. Overview on underground storage of natural gas. *Journal of Petroleum Technology*, *33*(06), pp.943-951.

Knepper, G.A., 1997. Underground storage operations. *Journal of Petroleum Technology*, *49*(10), pp.1112-1114.

Lemmon, E.W., Bell, I.H., Huber, M.L., McLinden, M.O. (2018). NIST Standard Reference Database 23: Reference Fluid Thermodynamic and Transport Properties-REFPROP, Version 10.0, National Institute of Standards and Technology, Standard Reference Data Program, Gaithersburg, doi: https" doi: https://doi.org/10.18434/T4/1502528

Luboń, K. and Tarkowski, R., 2020. Numerical simulation of hydrogen injection and withdrawal to and from a deep aquifer in NW Poland. *International Journal of Hydrogen Energy*, *45*(3), pp.2068-2083.

Luckner, L., Van Genuchten, M.T. and Nielsen, D.R., 1989. A consistent set of parametric models for the two-phase flow of immiscible fluids in the subsurface. *Water Resources Research*, *25*(10), pp.2187-2193.

Lysyy, M., Fernø, M. and Ersland, G., 2021. Seasonal hydrogen storage in a depleted oil and gas field. *International Journal of Hydrogen Energy*, *46*(49), pp.25160-25174.

Lysyy, M., Føyen, T., Johannesen, E.B., Fernø, M. and Ersland, G., 2022. Hydrogen relative permeability hysteresis in underground storage. *Geophysical Research Letters*, *49*(17), p.e2022GL100364.

Mouli-Castillo, J., Heinemann, N. and Edlmann, K., 2021. Mapping geological hydrogen storage capacity and regional heating demands: An applied UK case study. *Applied Energy*, *283*, p.116348.

Muhammed, N.S., Haq, B., Al Shehri, D., Al-Ahmed, A., Rahman, M.M. and Zaman, E., 2022. A review on underground hydrogen storage: Insight into geological sites, influencing factors and future outlook. *Energy Reports*, *8*, pp.461-499.

Muskat, M. and Wyckoff, R., 1935. :" An approximate theory of water-coning in oil production"./AIME Trans. Petr. Dev.

Nordbotten, J.M. and Celia, M.A., 2006. An improved analytical solution for interface upconing around a well. *Water resources research*, *42*(8).

Oldenburg, C.M. and Pan, L., 2013. Porous media compressed-air energy storage (PM-CAES): Theory and simulation of the coupled wellbore–reservoir system. *Transport in porous media*, *97*, pp.201-221.

Oldenburg, C.M., and S. Finsterle, iTOUGH2-EOS7CH: Simulation Capability for Hydrogen Storage in Porous Media Reservoirs, Finsterle GeoConsulting Report FGC-23-01, January 30, 2023.

Oldenburg, C.M., Moridis, G.J., Spycher, N. and Pruess, K. (2004). EOS7C Version 1.0: TOUGH2 Module for Carbon Dioxide or Nitrogen in Natural Gas (Methane) Reservoirs (LBNL-56589). Ernest Orlando Lawrence Berkeley National Laboratory, Berkeley, CA (US).

Pfeiffer, W.T. and Bauer, S., 2019. Comparing simulations of hydrogen storage in a sandstone formation using heterogeneous and homogenous flow property models. *Petroleum Geoscience*, *25*(3), pp.325-336.

Plaat, H., 2009. Underground gas storage: Why and how. *Geological Society, London, Special Publications*, *313*(1), pp.25-37.

Pruess, K., C. Oldenburg, G. Moridis (2012). TOUGH2 User's Guide, Version 2.1, Lawrence Berkeley Laboratory Report *LBNL-43134*, Berkeley, California.

Sáinz-García, A., Abarca, E., Rubí, V. and Grandia, F., 2017. Assessment of feasible strategies for seasonal underground hydrogen storage in a saline aquifer. *International Journal of Hydrogen Energy*, *42*(26), pp.16657-16666.

Saltelli, A., Ratto, M., Andres, T., Campolongo, F., Cariboni, J., Gatelli, D., Saisana, M., Tarantola, S., 2008. *Global Sensitivity Analysis: The Primer*. John Wiley and Sons, NewYork.

Sun, D. and Wong, P., 2017. Seawater upconing under a pumping horizontal well in a confined coastal aquifer. *International Journal of Environmental Sciences & Natural Resources*, *2*(1), pp.20-29.

Tarkowski, R. and Czapowski, G., 2018. Salt domes in Poland–Potential sites for hydrogen storage in caverns. *International Journal of Hydrogen Energy*, *43*(46), pp.21414-21427.

Thiyagarajan, S.R., Emadi, H., Hussain, A., Patange, P. and Watson, M., 2022. A comprehensive review of the mechanisms and efficiency of underground hydrogen storage. *Journal of Energy Storage*, *51*, p.104490.

Wainwright, H., S. Finsterle, Y. Jung, Q. Zhou, and J.T. Birkholzer, 2014. Making sense of global sensitivity analyses, *Computers & Geosciences*, *65*, 84–94, doi:10.1016/j.cageo.2013.06.006.

Wallace, R.L., Cai, Z., Zhang, H., Zhang, K. and Guo, C., 2021. Utility-scale subsurface hydrogen storage: UK perspectives and technology. *International Journal of Hydrogen Energy*, *46*(49), pp.25137-25159.

Wiles, L.E. and McCann, R.A., 1981. Water coning in porous media reservoirs for compressed air energy storage (No. PNL-3470). Battelle Pacific Northwest Labs., Richland, WA (USA).

Zhao, Y., McDonell, V. and Samuelsen, S., 2019. Influence of hydrogen addition to pipeline natural gas on the combustion performance of a cooktop burner. *International Journal of Hydrogen Energy*, *44*(23), pp.12239-12253.

Zivar, D., Kumar, S. and Foroozesh, J., 2021. Underground hydrogen storage: A comprehensive review. *International journal of hydrogen energy*, *46*(45), pp.23436-23462.

Statements and Declarations

Funding

This work was supported by a grant from EPRI to Finsterle GeoConsulting, LLC.

Competing Interests

The authors declare the following financial interests/personal relationships which may be considered as potential competing interests:
Curtis M. Oldenburg and Stefan Finsterle report financial support was provided by Electrical Power Research Institute (EPRI), Palo Alto, California, USA.

Author Contributions
Oldenburg, Finsterle, and Trautz contributed to problem conceptualization. Oldenburg and Finsterle developed the methodology and carried out the formal analysis and simulations. Oldenburg and Finsterle wrote the original draft. Trautz was project administrator, and carried out review and editing.

Data Availability
Not applicable